

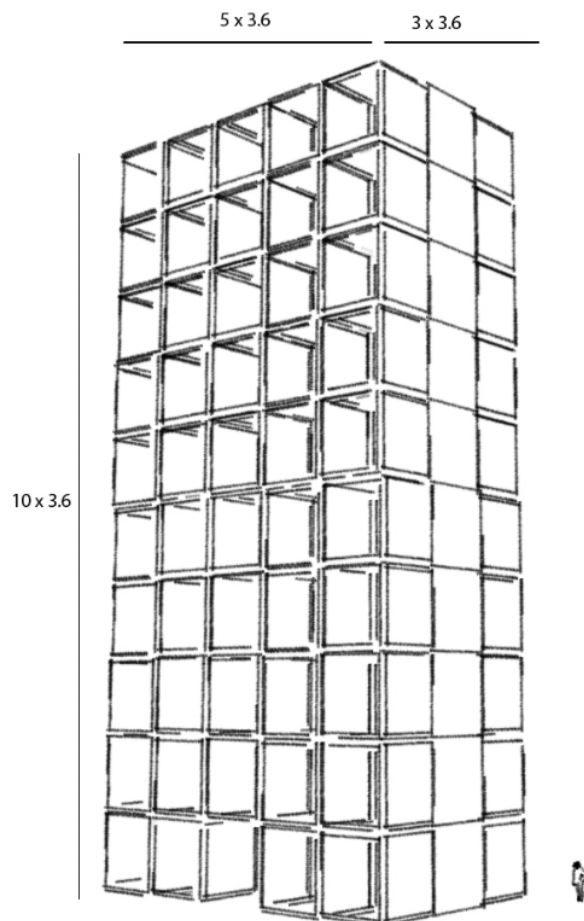
Structural design of multi-story modular building with emphasis on sustainability

Master Thesis

10th June, 2020

Author:
Matúš Uriček

Supervisor:
Christian Frier





AALBORG UNIVERSITET
STUDENTERRAPPORT



AALBORG UNIVERSITET
STUDENTERRAPPORT

The Faculty of Engineering and Science
Structural & Civil Engineering
Thomas Manns Vej 23
9220 Aalborg SØ
<http://www.civil.aau.dk>

Title:

Structural design of multi-story modular building with emphasis on sustainability

Project:

MSc Short Master Project

Project period:

January 20th 2019 - June 10th 2020

Author:

Matúš Uriček

Supervisor:

Christian Frier

Pages: 50

Appendix: 5

Finished 10-6-2020

Abstract:

The project addresses problems of stagnating construction industry, scarcity of affordable housing and plastic pollution. Innovative production technology is introduced, which uses industrial waste plastic, more specifically polyoxymethylene (POM). The manufacturing process combines continual extrusion and additive manufacturing.

Corner supported modular system with stiff modules is adopted. The modules are fully produced, assembled and outfitted off-site, in controlled environment. This allows mass production and mass customization of the modules, which decreases manufacturing costs. More affordable houses of superior quality can be produced.

Several versions of multi-story buildings are designed and analysed. Load acting on the structures are calculated and their effects analysed. Based on that, structural elements are designed. Emphasis is put into stiffness of the structure, due to relatively low stiffness of the POM material. Therefore, serviceability limit state is determining. For taller buildings, steel bracing rods are used to provide structural stiffness.

Joints between the structural elements and modules are designed so they allow complete disassembly. This provides a benefit that the modules can be reused, used as self-standing structures, reallocated and at the end of the lifetime easily recycled.

Preface

This Master thesis project in Structural and Civil Engineering (Master) at Aalborg University has been written by Matúš Uriček. The report has been written from December 2019 till 10th June 2020. The semester project consists of the main report and an appendix where extra documentations are located. The main report is divided in parts that include the chapters corresponding to the described topics. The chapters for the appendix are named by the letters of alphabet, written as A.1, A.2, B.1, B.2... when making the reference to the appendix during the report.

Reading guide

The report uses the harvard-method literature reference, where sources that are used refers to the author's last name and the year of the publication in brackets - Surname [Year]. Tables and figures produced by the author have no sources. In case of a figure or table taken from a source, but which has been modified by the author, a reference to the source is written with the same reference format as mentioned above.

Tables, figures and equations are numbered by chapter, number and location in the chapter.

Matúš Uriček

Summary

This thesis responds to several problems of the construction industry and human society in general. For several decades the construction industry has been stagnating and is late to adopt modern production technologies. Construction of one-off buildings produced with traditional techniques becomes unsustainable as the skilled workforce is aging and the jobs are unattractive for younger generation. Moreover, construction industry produces high amounts of *CO2* emissions and waste. Most production materials are down-cycled after the lifetime of the structure.

Innovative production technology is introduced, which combines extrusion and additive manufacturing. The production material is plastic up-cycled from industrial waste. The material is polyoxymethylene (POM), an engineering plastic with relatively low sensitivity to creep and high temperatures. Advantages are high durability and workability. Furthermore, at the end of the lifetime the material can be reused and recycled.

Modular construction approach is adopted, where modules are mass produced off-site. Factory environment provides stable conditions, effective quality control loops and more attractive job opportunities. Advanced manufacturing technologies are more easily adopted. Production costs are decreased which enables reinforcement of the affordable housing market.

Case study of multi-storey modular buildings is conducted. First, loads acting on the structures are evaluated, including construction loads induced on modules during execution. Then, based on the calculated loads, structural elements are designed and analysed. Serviceability limit state is the design criterion due to relatively low stiffness of the material. Due to that, most of the structural material is not used effectively. This is favorable as robust structure is needed while effects of the production technology on the used material are unknown.

Corner supported modular system with stiff modules is adopted. This system doesn't contain a structural core. Therefore, the whole building is modular and can be disassembled in the same way in which it was assembled. Taller buildings are reinforced with steel bracing rods. The production technology allows creation of internal channels into which the bracing rods can be inserted. They connect corners of the stiff modules, where they are anchored with use of nuts and washers. The stiff modules provide lateral stability and stiffness for the whole building.

Finally, structural joints are designed which connect structural elements and adjacent modules. Mechanical joints consisting of bolted connections are used as they allow complete disassembly of the structure. The modules of the structure can be used separately, incorporated in a different structure or the original structure can be reallocated. This system can react to fluctuations of demand and provide temporary housing in times of crisis.

List of acronyms

POM	polyoxymethylene
POM-C	polyacetal - copolymer
AM	additive manufacturing
LSAM	large scale additive manufacturing
FDM	fused deposition molding
FFF	fused filament fabrication
WEF	World Economic Forum
CTF	Construction Task Force

Table of Contents

Chapter 1 Introduction	1
1.1 Problem statement	1
1.2 Off-site manufacturing	1
1.3 Modular construction	2
1.4 Standardization and mass customization	4
1.5 Aims and objectives	4
Chapter 2 Manufacturing specifications	6
2.1 Manufacturing technology	6
2.2 Additive manufacturing machine	8
2.3 Production constraints	8
2.4 Material	9
2.5 Anisotropic material properties	10
2.6 Long-term material behavior	10
Chapter 3 Actions on structures	12
3.1 Layout of the buildings	12
3.2 Self-weight	14
3.3 Imposed loads	16
3.4 Snow loads	17
3.5 Wind loads	18
3.6 Actions during execution	23
Chapter 4 Structural design	25
4.1 Floor element	25
4.2 Roof element	29
4.3 Column	31
4.4 Lateral stiffener	35
Chapter 5 Structural connections	41
5.1 Intra-module connections	41
5.2 Inter-module connections	48
Chapter 6 Conclusion	50
Bibliography	51
I Appendix	52
Appendix A POM Datasheet	53
Appendix B Creep curves for POM	54

Appendix C Wind Loads

56

1.1 Problem statement

The construction industry is stagnating (or is developing slower) in context of its effectiveness and profitability in contrast to other industries which exhibit rapid and constant improvement. Margins are characteristically too low for the industry to sustain healthy development and therefore it invests little in research and development and in capital. Furthermore, there is a crisis in training as too few people are being trained to replace the ageing skilled workforce. The construction industry is considered to be under-achieving, both in terms of meeting its own needs and those of its clients, (CTF [1998]).

This slow pace of innovation matters, because of the great scale of the construction sector. The industry accounts for about 6% of global GDP and is growing. Construction industry is the largest consumer of raw materials and other resources, using about 50% of global steel production and more than 3 billion tonnes of raw materials. Any improvement in productivity and successful adoption of modern innovative processes will have a major impact. For example, a 1% rise in productivity worldwide could save \$100 billion a year. Yet, the overall productivity in the sector has remained nearly flat for the last 50 years, (WEF [2016]).

One approach to address the inefficiencies of construction industry is the use of off-site manufacturing and modular construction. It is a way to shift a part of the construction work into a manufacturing environment, where some of the production processes can be executed in more effective way, e.g. by automatizing them, and with higher processing quality, while preparatory on-site work can be accomplished in parallel. This leads to quantifiable economic and sustainability benefits.

This project also addresses the problem of plastic waste (state numbers of the amounts globally) as the main structural material of a proposed modular design is recycled plastic. The structural components of modules will be manufactured additively with use of Big Area Additive Manufacturing (BAAM) technology.

1.2 Off-site manufacturing

Off-site manufacturing or fabrication is a production process which incorporates prefabrication and pre-assembly. These processes generally take place in a specialized facility, where various materials, components and eventually equipment are joined together in order to complete a proportion of the building's final assembly work before installation in its final position, (Gibb [1999]).

Essentially, according to Lawson [2014], these construction methods transfer (/delegate) repetitive

and/or unproductive site activities into factory environment, where they can be executed in more efficient and faster way. However, this necessitates greater investments into fixed manufacturing facilities and a repeatability of the tasks in order to utilize an economy of scale in production.

The main types of off-site fabrication can be defined by the following categories, (Lawson [2014]):

- Modular construction—Three-dimensional or volumetric units that are generally fitted out in a factory and are delivered to the site as the main structural elements of the building.
- Planar construction—Two-dimensional panels, used mainly for walls, that can be pre-finished with their insulation and boarding attached before delivery to the site.
- Hybrid construction—Mixed use of linear elements, panels, and modules to create a mixed-construction system.
- Cladding panels—Prefabricated façade elements that are attached to the building to form the completed building envelope.
- Pods—Nonstructural modular units, such as toilets and bathrooms, that are supported directly on the floors of the building.

The focus of this report is oriented towards modular construction, where the amount of on-site work is minimized.

1.3 Modular construction

As stated in the previous section, modular construction utilizes three-dimensional or volumetric units. Dimensions of the units are limited by the requirements of a transportation system and typically there is a tendency to produce units which are as large as possible. Generally, one unit contains a whole room, or partially or fully open units can be combined to form larger spaces. The units are usually fully finished in factory environment and assembled on-site to form complete buildings or their major parts.

Initially, modular construction was used mainly in areas of temporary and/or portable buildings. Nowadays, the construction technology is used for many types of buildings as schools, hospitals, offices and high-rise residential buildings. In general, it is used in sectors with high level of repetitiveness or service integration, or where there is a need for fast construction or low disturbance of the building process.

According to Christopher Nash (Grimshaw Architects LLP), modular construction should not be seen as a structural or architectural approach, but rather as a means of delivery that can favor certain building design concepts, but most importantly it should be seen as a procurement process. It is a way of thinking about construction which seeks to bring the construction of buildings onto a more sophisticated footing.

1.3.1 Advantages of modular construction

The key benefits of modular construction are:

- Rapid construction—Shorter build times are achieved by parallelization of processes, which leads to smaller disturbance of the adjacent area, better social impact, reduced site management costs and faster return on the investment.
- High quality—Factory-based fabrication processes and production checks lead to superior quality.

- **Economy of scale**—Achieved in repeated or/and larger projects, with use of the same module design multiple times.
- **Economic benefits**—Use of modular construction leads to decreased total costs, due to increased productivity, effectiveness, decreased design costs and through economy of scale.
- **Sustainability**—Factory production leads to decreased wastage and material use, and better opportunities for recycling.
- **Safety**—Significant reduction of work at heights, dry and warm conditions of the factory environment, on-site work limited to specialized installation team.
- **Greater reliability**—Higher probability of project completion on time, greater reliance on the outcome and smaller chance of production faults.
- **Ability of the building to be dismantled and reused**—Asset value of the building can be maintained also after loss of demand at the location, modules or their elements can be reused in different buildings and recycling is simplified.
- **Excellent acoustic insulation and fire safety**—Effective isolation of side to side and above and below modules due to double-skin nature of the construction.

The modular construction is a suitable choice in the cases, where it is possible to put a business value to the aforementioned benefits. On the other hand, the construction technology requires more elaborated communication and coordination among all members of the design and construction team, more extensive planning and higher initial capital for the construction company in order to establish the necessary facilities.

1.3.2 Categorization of modular construction

Modules used in modular construction can be categorized according to their load transfer mechanism:

- **Load bearing modules**—Loads are transferred through side walls of the modules into the foundation. They are mainly used for 1 and 2 storey buildings.
- **Corner supported modules**—Loads are transferred from the longitudinal edge beams into the supporting corner columns and subsequently into the foundation or a podium floor. These modules can be used for taller buildings.

Modular buildings can be categorized based on the used structural system:

- **Load bearing system**—Usually one to two storey buildings, consisting of load bearing modules described above. The modules and their interfaces are not designed to transfer lateral loads between the modules.
- **System containing central core**—Lateral loads are transferred by central core into the foundation. Central core is usually fabricated on-site and made of reinforced concrete. Therefore, this system can not be seen as fully modular. Corner supported modules are connected to the central core either directly or through neighbouring modules. Another way to transfer lateral loads from modules to central core, sometimes used in practice, is to fill horizontal gap between the roofs and floors of certain level modules with concrete. This creates a continuous diaphragm, which is connected to the core. The systems containing central core has been used for building more than 30 stories high.
- **Corner supported modular system with stiff modules**—Self-sustained system in which sufficient lateral resistance is ensured by strategically placed stiff modules. The buildings with this structural system can be seen as purely modular.

Another categorisation concerning modular structures can be based on the construction material used in their load bearing structure. Materials which already have been used are steel, concrete, timber and glass fibre reinforced polymers. This report investigates use of recycled plastic as the structural material of the modules, which are fabricated with use of additive manufacturing.

In the scope of this project, corner supported modular system with stiff modules will be used, as this system can be used in high-rise buildings. This system can be seen as purely modular, which enables full exploitation of the benefits of modular structures. Namely in the domain of sustainability, as buildings with this structural system can be dismantled and reused.

1.4 Standardization and mass customization

Benefits of modular construction can be realized in higher extend when it is combined with standardization. Here, by standardization is meant a voluminous use of construction parts and components with high level of repetition and regularity, where there also might be a history of successful practise. Mainly interfaces between modules should be standardized in order to allow their interchangeability and increase freedom of the overall design. Modules can benefit from advances in manufacturing industry and mass customization can be used rather than simple mass production, (Gibb [1999]).

Construction industry, in contrast with other industries, traditionally demands for one-of-a-kind products, in order to achieve distinctive architecture and fulfill a specific function in various environments. This is one of the reasons why construction industry experiences smaller degree of industrialization. This obstacle can be bridged with use of mass customization. Mass customization typically makes use of flexible manufacturing systems and enables industrial production of large batch of customized products at low cost. These principles bring great potential into construction industry, (Jensen [2015]).

1.5 Aims and objectives

There is a substantial knowledge gap in the area of modular construction due to relative novelty of the technology. Especially medium to high rise multi-story buildings, subjected to significant lateral loads, seems to be structurally over-designed in order to ensure safe design despite the incomplete understanding of the structural behavior. Further, use of additive manufacturing in construction industry is mostly unexplored field.

This project aims to further the understanding of the structural behavior of multi-story modular buildings. As emphasis is given to sustainability of the design, focus will be oriented towards corner supported modular system with stiff modules, mentioned in Section 1.3.1. This structural system exploits potential of the modular construction, namely rapid construction due to paralelization of the construction processes and capability to be disassembled, reused and effectively recycled.

Structural behavior of additively manufactured structural elements made of recycled plastic will be elucidated. In the case of this type of structure, manufacturing specifications need to be carefully specified as they highly influence material properties. Especially anisotropy of the material needs to be taken into account as it can highly influence the structural behavior of the modules.

Connections between the modules have to transfer lateral and vertical loads effectively. Therefore, they play a significant role in the overall structural behavior of the modular system. They need

to be analyzed in higher detail with aim to understand the manner in which they influence the structural behavior globally. In doing so, it may be possible to further optimize the structural system and the connections themselves.

In order to fulfill these aims, exemplary multi-story modular buildings are designed and analyzed in the scope of this project. Emphasis is given towards the sustainability of the design. Following objectives will guide the approach:

- Preliminary design of the modular buildings and estimation of the vertical and lateral loads acting on the load bearing structures.
- Identification of the overall structural behavior of the modular systems subjected to vertical and lateral loads and analysis of the load transfer mechanisms.
- Design and analysis of the additively manufactured modules.
- Detailed analysis of the connections between modules and description of their contribution to the load transfer mechanism.

Manufacturing specifications

2

This chapter specifies the manufacturing method which will be used for production of the load bearing structure, the used material and implications of the used manufacturing method on the behavior of the material.

2.1 Manufacturing technology

Manufacturing technology used for the production of load bearing structure is combination of extrusion and additive manufacturing. The production process is fully automatic and consists of the following steps:

- Extrusion of the edge sheets
- Cutting and machining of the sheets into desirable shapes
- 3D printing of the infill structure on the prepared sheets
- Insertion of insulation and mechanical systems into the panels
- Closing the panels with second sheet

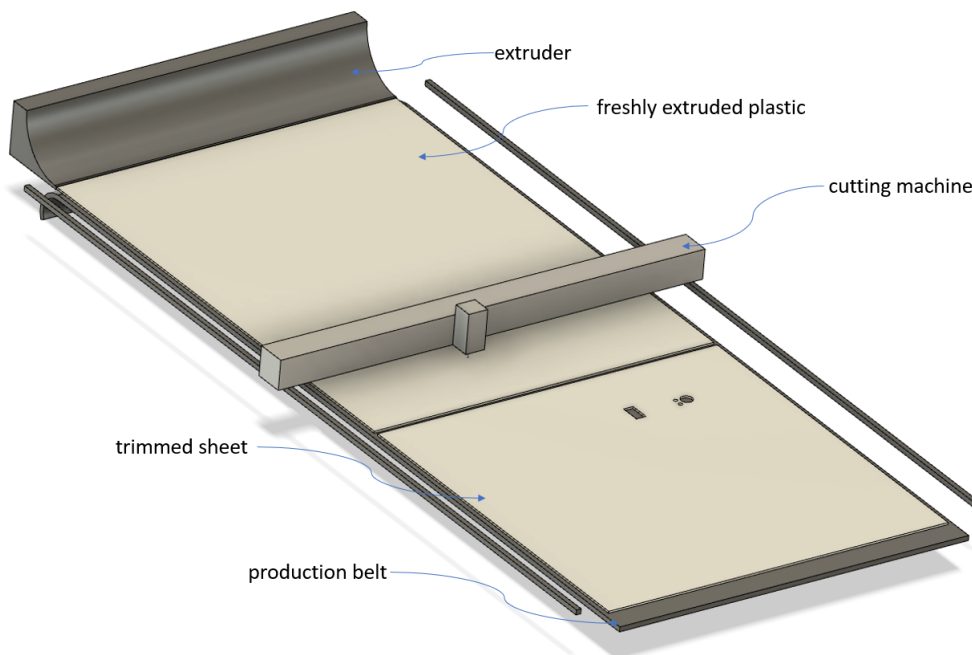


Figure 2.1: Extrusion and cutting of the edge sheets

Figure 2.1 describes first two steps of the production process, extrusion and cutting of the edge

sheets. Raw material in form of pellets enters the extruder, here it is melted and pushed through a nozzle. The material cools down and is trimmed into a desirable shape.

Next step is 3D printing of the infill structure. This process is represented by Figure 2.2. The infill structure is printed directly on the edge sheet.

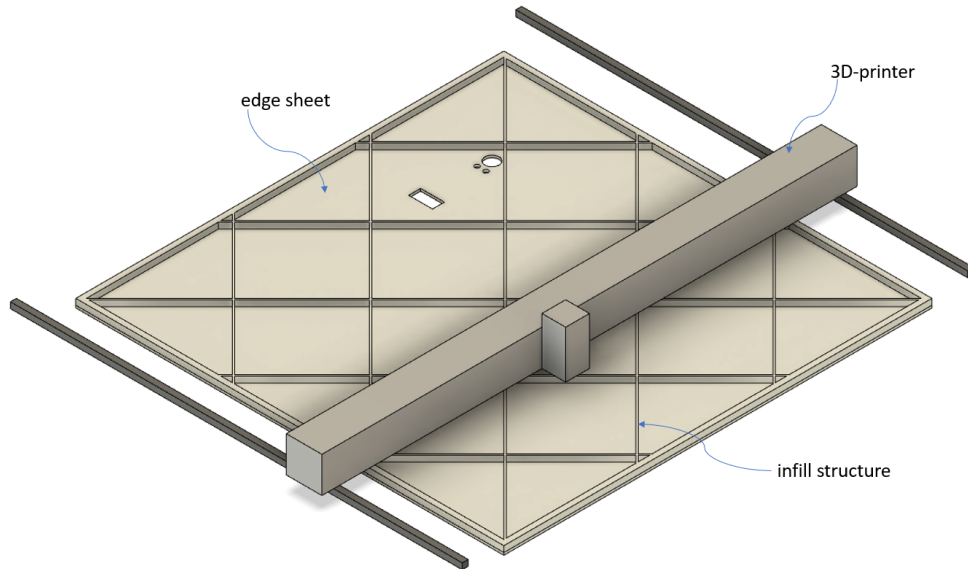


Figure 2.2: 3D printing of the infill structure

The next step is insertion of mechanical systems and filling the spaces between the infill structure with insulation. Then, the panel is closed by bonding another edge sheet to the infill material. The assembly is shown on Figure 2.3.

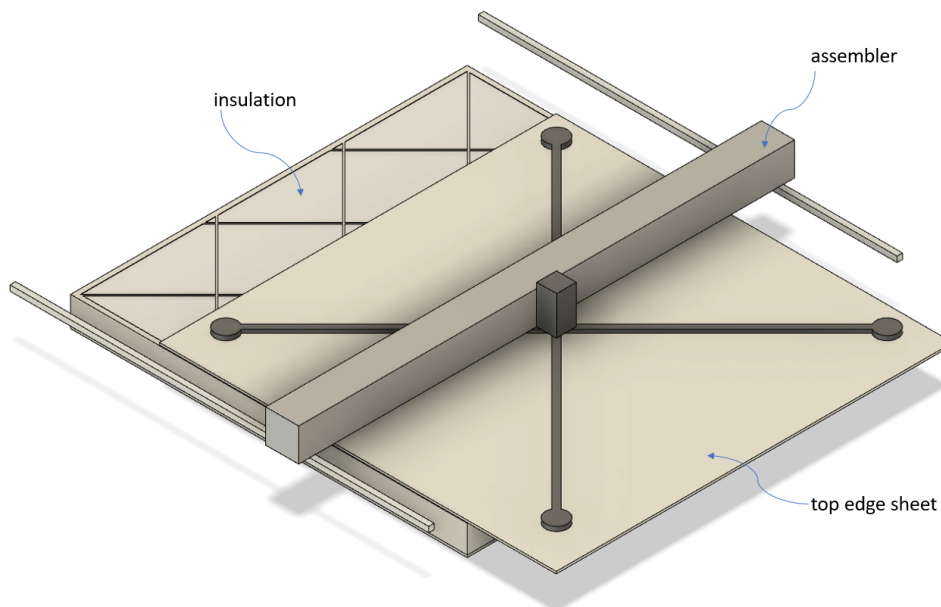


Figure 2.3: 3D printing of the infill structure

2.2 Additive manufacturing machine

The additive technology used for production of the structural elements is termed Large Scale Additive Manufacturing (LSAM) which in principle is similar to fused filament fabrication (FFF). The difference is in the scale of the production rig and its components. The principle of this technology is that plastic pellets are fed into an extruder, where it is heated slightly above the melting point of the used material. The melted material is then pushed out of the extruder through a nozzle and placed on a production plate or an unfinished part. A whole layer of a part is created by computationally controlled movements of the extruder in horizontal plane. After one layer is finished, the extruder moves up for a distance equal to the pre-designed layer height. The process continues until the whole component is finished.

The infill of the structural elements of the modules will be manufactured with use of a customized 3D printer, whose draft is shown on Figure 2.2. The working area has a length and width of 4 meters and the range of the extruder's vertical movement is 50 cm. The printer allows production of planar structural elements, such as walls, roofs and floors and linear members, such as beams and columns.

2.3 Production constraints

One of the main construction constraints is the maximal size of a structural element which is limited by the size of the production rig. The maximum length and width of the structural elements is 4 meters and thickness is 0.5 meters.

Further, production constraints are connected to the limitations of the additive manufacturing technology. First, the nozzle through which the printed material is pushed creates beads with specific width and height. The cross-section of the bead can be modulated by controlling the speed of extrusion. However, in this report we consider a constant cross-section of the bead with a width of 15 mm and height of 6 mm. These dimensions need to be taken into account in the design of the infill structure. Parts of the infill structure must have a size which can be obtained by multiplication of the dimensions of the bead. The size of the bead is shown on Figure 2.4.

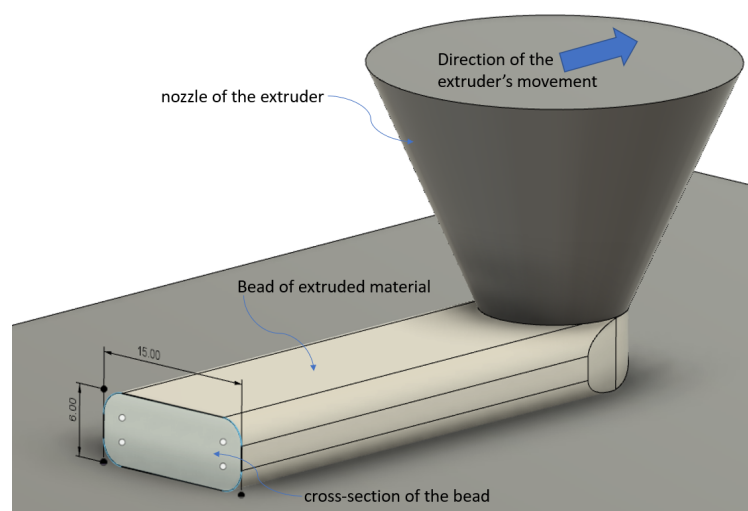


Figure 2.4: Bead of the extruded material

Another constraint is that material can not be extruded on top of void. In small scale additive manufacturing it is possible to bridge voids of limited length, but it is not possible in the case of LSAM. In LSAM, material can be extruded only on top of existing material.

2.4 Material

The material used for the production of the load-bearing structure is polyoxymethylene (POM), also known as acetal. Specifically, POM up-cycled from an industrial waste material is used. The waste material is first minced and then remelted and formed into pellets. The pellets are then fed directly into the extruder of the AM machine.

POM is a crystalline thermoplastic generally accepted as an engineering material and often termed as an engineering plastic. Definition which can be used for engineering material is that it can support loads more or less indefinitely. In this regard, POM has several disadvantages when compared with metals. For example, it has low time-dependent stiffness modulus and its mechanical properties are sensitive to ambient temperature. However, important advantages of POM are its low density, chemical resistance and most importantly, easy processability, thanks to which it can be easily formed into complex shapes, (Crawford [1998]).

Mechanical properties of POM are in many respects similar to those of nylon and they can be used for the same type of light engineering applications. Advantage of POM in comparison to nylon is its low water absorption, disadvantage might be its higher density. POM is available as a homopolymer and a copolymer. The copolymer has improved high temperature performance and it is the type used in the scope of this project.

Exact properties of the POM material depend on manufacturer. The raw material was produced by company Ensinger. The factory name of the material is TECAFORM AH-natural and its detailed data-sheet is shown in Appendix A. Main properties extracted from this data-sheet are listed in Table 2.1.

Table 2.1: Properties of the used POM material

E_t	Modulus of elasticity (tension)	2800 MPa
E_f	Modulus of elasticity (bending)	2600 MPa
E_c	Modulus of elasticity (compression)	2300 MPa
S_y	Tensile strength at yield	67 MPa
ϵ_y	Elongation at yield	9 %
ϵ_u	Elongation at break	32 %
G	Shear modulus	930 MPa
ν	Poisson's ratio	0,39 –

Values of shear modulus, G , and poisson's ratio, ν , were obtained from Crawford [1998].

2.5 Anisotropic material properties

The FFF additive manufacturing machine deposits the material in a directional way which produces structures with anisotropic behavior. The extruded material has various properties in the direction of the beads and direction perpendicular to the beads, where the mechanical behavior is governed by adhesion of the beads, either next to each other or on top of each other.

The manufacturing parameters which can affect the mechanical properties of the produced material are:

- Orientation of the beads relative to the loading direction
- Temperature of the extruded material
- Space between the immediate lateral beads

According to Sung-Hoon [2002], the mechanical behavior in tension of the material produced with FFF technology is affected mostly by size of the spaces between the beads and their direction. The space between the beads should be defined as negative, so that the beads merge together and the strength across the beads is decreased minimally. Further, if a cross raster is used (beads in perpendicular directions according to each other in the immediate layers on top of each other), the tensile strength is decreased. If the orientation of the beads is $[0^\circ/90^\circ]$, the tensile strength is decreased by 28%. If the orientation of the beads is $[45^\circ/-45^\circ]$, the tensile strength is decreased by 35%. Therefore, the structure should be designed in a way, so that the tensile loads are carried along the beads. The compressive strength is not affected much by the build direction and hitherto this effect will be neglected.

In order to be on the safe side the design value of the tensile strength is decreased by 35%. The value of tensile strength of the POM material used for the design purposes is then 43 MPa.

2.6 Long-term material behavior

POM is a viscoelastic thermoplastic material. Therefore, when the material is stressed it reacts by exhibiting viscous flow (energy dissipation) and elastic displacement (storing of energy). The properties of this material are dependent on time, temperature and strain rate.

The time dependent properties of POM material are characterised by creep curves presented in Appendix B. The lifetime of the structure is designed as 40 years. However, none of the creep curves show data for such long time period. An approximation of the creep behavior after 40 years can be found by extrapolation of the creep curves on Figure B.3. Then an apparent stiffness modulus can be calculated by:

$$E_{app,40} = \frac{\sigma}{\epsilon_{40}} \quad (2.1)$$

Where

$E_{app,40}$	Apparent stiffness modulus after 40 years
σ	Stress in the material
ϵ_{40}	Strain after 40 years for given stress

The apparent stiffness modulus, $E_{app,40}$, does not represent actual stiffness of the material, it is just a parameter for calculation of the strains and deflections after 40 years of loading. It is found out that the apparent stiffness modulus, $E_{app,40}$, for all the curves on Figure B.3 is approximately 670MPa. Therefore, this value is used for calculation of long-term behavior of the POM material.

Actions on structures

3

This chapter defines the modules and the layouts of the buildings under consideration consisting of these modules. Then calculation of loads on these buildings is conducted.

3.1 Layout of the buildings

The buildings under consideration consist of modules which are cube-shaped. The sides of the cubes are 3.6 metres long. The modules are connected together to form storeys. One storey is 5 modules wide and 3 modules deep. An example of a footprint of such a storey is shown on Figure 3.1.



Figure 3.1: Example of a storey footprint

There are four basic types of modules under consideration, represented by letters R, C, E and S on Figure 3.1. R stands for residential module, C for common module, E for elevator module and S for staircase module. Residential modules provide habitation for single tenants. Common modules form common areas for adjacent residential modules. Elevator and staircase modules provide vertical transportation. Elevator module also contain shaft for vertical distribution of mechanical grids.

One of the qualities of modular construction is that the modular buildings can be disassembled and the modules used in different applications. Therefore, the residential modules are designed also for the case of them being used as self-standing structures. That means the residential modules must have inherently high stiffness and will therefore act as the stiff modules of the buildings to form the corner supported modular system with stiff modules described in Section 1.3.2. The geometry

of the residential module is represented on Figure 3.2. The thickness of the walls is set to 200mm and height of the floor and roof elements is limited to 300mm. One side of the module is designed to be fully open to incorporate a large window. This side of the module is not considered to carry any load. The opposite side of the the module includes opening for entrance door.

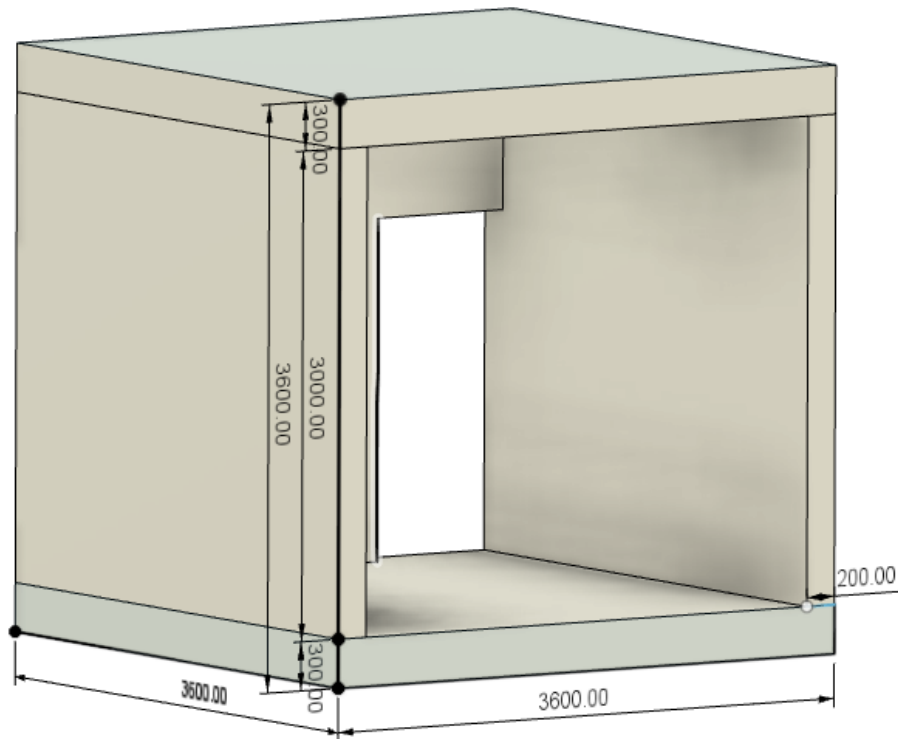


Figure 3.2: Residential module

The multi-storey structures are then formed by stacking the storeys represented by Figure 3.1. Buildings consisting of 1, 2, 3, 4, 5 and 10 such storeys are considered. Their layouts are shown on Figures 3.3, 3.4, 3.5, 3.6, 3.7 and 3.8.

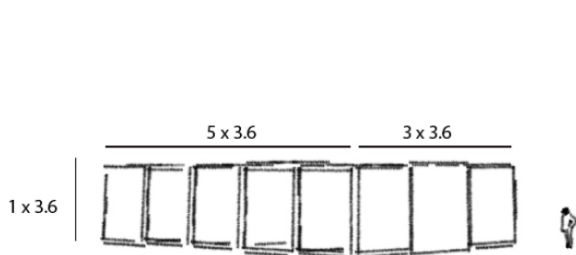


Figure 3.3: 1-storey building

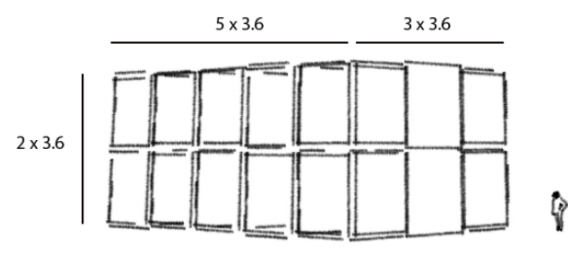


Figure 3.4: 2-storeys building

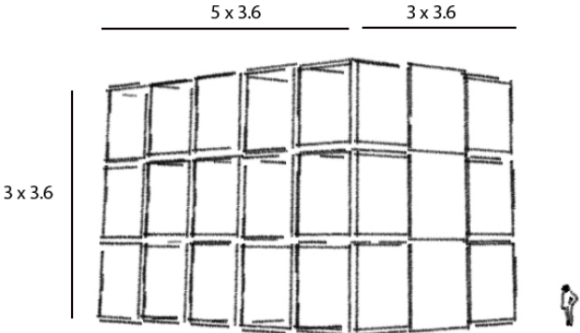


Figure 3.5: 3-storeys building

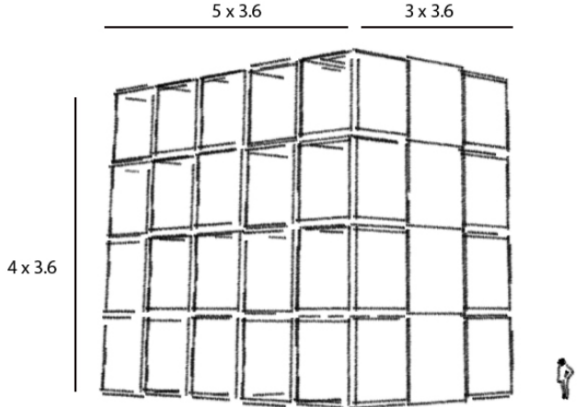


Figure 3.6: 4-storeys building

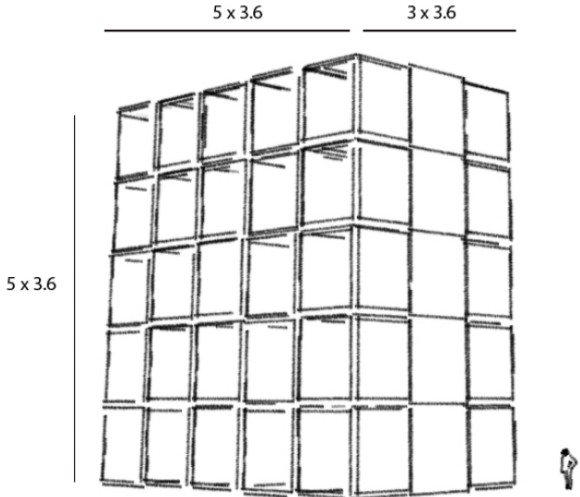


Figure 3.7: 5-storeys building

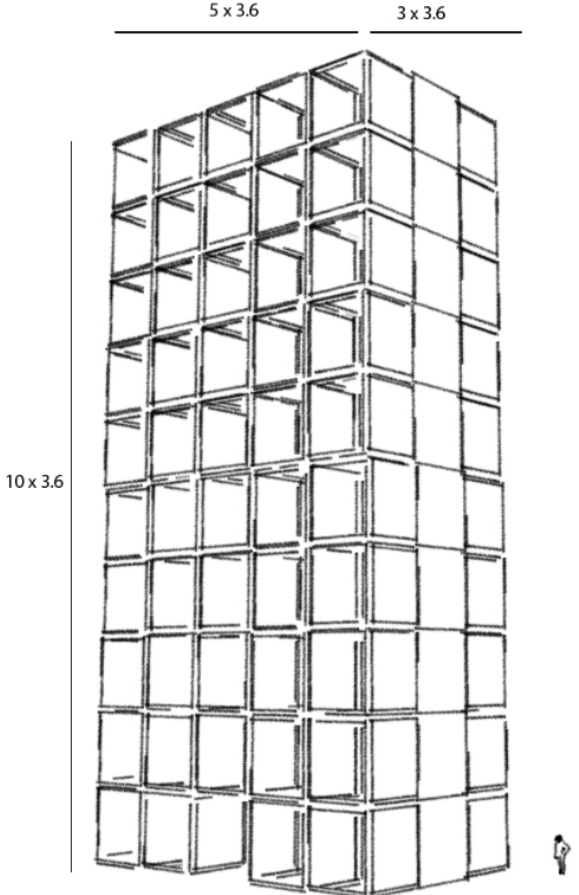


Figure 3.8: 10-storeys building

3.2 Self-weight

The additive manufacturing technology is capable of creation of internal infill structure. This structural pattern increases effectiveness of the used material and creates hollow spaces inside of

the elements. This spaces can be filled with insulation to improve thermal properties of the elements.

Further, self-weight of the structural elements is estimated, based on the weights of the raw materials: $14,1 \frac{\text{kN}}{\text{m}^3}$ for POM and $1,5 \frac{\text{kN}}{\text{m}^3}$ for perlit insulation.

3.2.1 Floor

Figure 3.9 shows cross-section of unit length of floor element. The vertical internal walls represent the internal infill structure. The estimated weight of the flooring is $0,25 \frac{\text{kN}}{\text{m}^2}$. The volume of POM material needed for construction of floor element is estimated to $0,06 \text{ m}^3$ per m^2 of the floor. Then the self weight of the floor element per m^2 , g_f , can be calculated as:

$$g_f = 0,035 \frac{\text{m}^3}{\text{m}^2} * 14,1 \frac{\text{kN}}{\text{m}^3} + 0,265 \frac{\text{m}^3}{\text{m}^2} * 1,5 \frac{\text{kN}}{\text{m}^3} + 0,25 \frac{\text{kN}}{\text{m}^2} = 1,141 \frac{\text{kN}}{\text{m}^2} \quad (3.1)$$

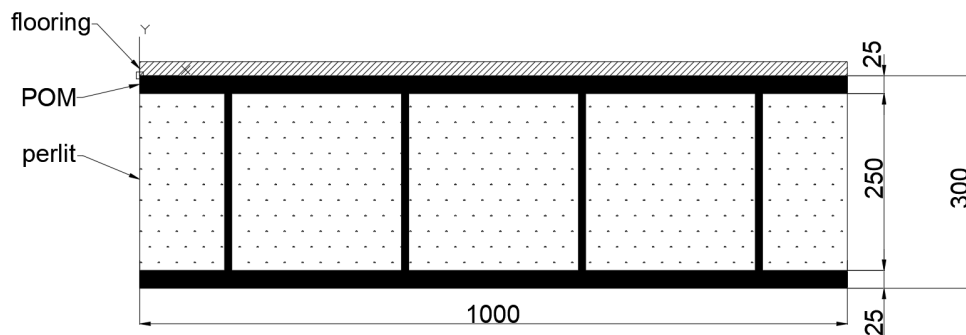


Figure 3.9: Cross-section of unit length of floor element

3.2.2 Roof

The cross-section of the roof element, shown on Figure 3.10, is similar to the cross-section of floor element. The difference is in the amount of structural material, as roof element is expected to be loaded less, and the absence of flooring. The self weight of roof element per m^2 , g_r , is calculated as:

$$g_r = 0,04 \frac{\text{m}^3}{\text{m}^2} * 14,1 \frac{\text{kN}}{\text{m}^3} + 0,27 \frac{\text{m}^3}{\text{m}^2} * 1,5 \frac{\text{kN}}{\text{m}^3} = 0,969 \frac{\text{kN}}{\text{m}^2} \quad (3.2)$$

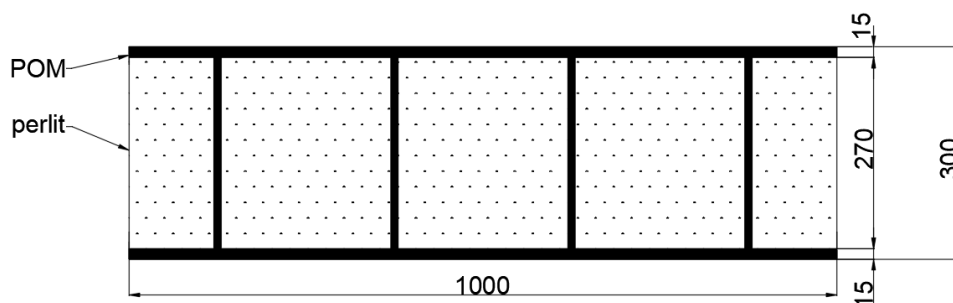


Figure 3.10: Cross-section of unit length of roof element

3.2.3 Wall

The wall element is not expected to be load bearing, unless it is acting as a shear wall, in which case it needs to be designed specifically for that purpose. Therefore, less structural material is expected to be used for the wall element, as seen on Figure 3.11. Then the estimated self weight of square meter of the wall, g_w , is calculated as:

$$g_w = 0,03 \frac{\text{m}^3}{\text{m}^2} * 14,1 \frac{\text{kN}}{\text{m}^3} + 0,18 \frac{\text{m}^3}{\text{m}^2} * 1,5 \frac{\text{kN}}{\text{m}^3} = 0,693 \frac{\text{kN}}{\text{m}^2} \quad (3.3)$$

While the wall is a vertical element, it is useful to calculate its self-weight per length of the wall, $g_{w,l}$, as it is acting on its bottom edge. This is simply done by multiplying the self-weight per m^2 by the height of the wall:

$$g_{w,l} = 0,693 \frac{\text{kN}}{\text{m}^2} * 3 \text{ m} = 2,08 \frac{\text{kN}}{\text{m}} \quad (3.4)$$

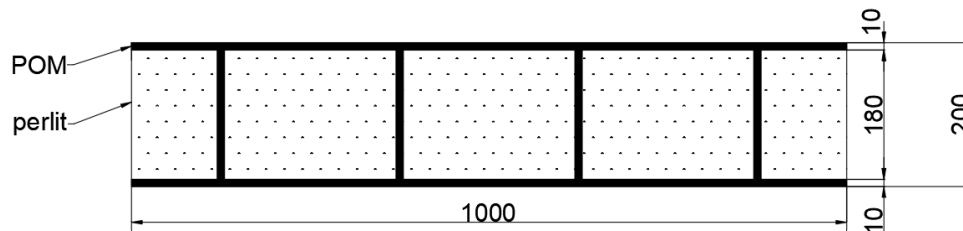


Figure 3.11: Cross-section of unit length of wall element

3.2.4 Column

The self weight of the column, G_c , is perceived as a point load acting in the corner of the floor element. Then, it is calculated as the volume of the column, represented by Figure 3.12, times the weight of the POM material. In principle, hollow section of the column could be used, but here the calculation is conducted for solid cross-section:

$$G_c = 0,2 \text{ m} * 0,2 \text{ m} * 3 \text{ m} * 14,1 \frac{\text{kN}}{\text{m}^3} = 1,692 \text{ kN} \quad (3.5)$$

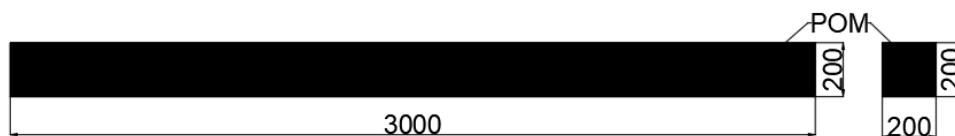


Figure 3.12: Side view and cross-section of column element

3.3 Imposed loads

This section is based on Eurocode EN1991-1-1:2002 [2010].

Imposed loads are the loads arising from occupancy of the building. This includes normal use by persons and weight of furniture and movable objects. The imposed load should be taken as a free

action applied at the most unfavorable part of the influence area. When the imposed loads from other storeys are considered, they may be assumed as uniformly distributed. A separate verification shall be performed with a concentrated load to ensure a minimum local resistance.

According to use of the building, it belongs to category A - Areas for domestic and residential activities. For this category, the recommended characteristic values of the imposed loads are shown in Table 3.1.

Table 3.1: Imposed loads

Category A	$q_k [\frac{kN}{m^2}]$	$Q_k [kN]$
Floors	2	2
Stairs	2	2
Balconies	2.5	2

Where

q_k		Characteristic value of uniformly distributed load for determination of general effects
Q_k		Characteristic value of concentrated load for determination of local effects

The self-weight of movable partitions can be added to the imposed loads of floors as a uniformly distributed load q_k . The partitions considered for the building have self-weight of less than $1 \frac{kN}{m}$ for which $q_k = 0,5 \text{ kN/m}^2$ can be used.

Where imposed loads from several storeys act on columns and walls, the total imposed loads may be reduced by a factor α_n . The reduction factor α_n is calculated as:

$$\alpha_n = \frac{2 + (n - 2)\psi_0}{n} \quad (3.6)$$

Where

n		The number of storeys (>2) above the loaded structural elements
ψ_0		Factor, for category A equal to 0.7

Values of α_n for selected number of storeys are shown in Table 3.2.

Table 3.2: Values of reduction factor α_n

n - number of storeys	α_n - reduction factor
3	0.9
4	0.85
5	0.82
10	0.76

3.4 Snow loads

This section is based on Eurocode EN1991-1-3:2003 [2010].

The snow loads should be assumed to act vertically and refer to a horizontal projection of the roof area. Snow loads on roofs shall be calculated with the following equation:

$$s = \mu_i C_e C_t s_k \quad (3.7)$$

Where

μ_i		Snow load shape coefficient
C_e		Exposure coefficient
C_t		Thermal coefficient
s_k		Characteristic value of snow load on the ground

The building might be build in a sheltered topography or such topography might be created by future development around the site. Therefore, the exposure coefficient is taken as $C_e = 1.2$.

The roof of the buildings is considered to have low thermal transmittance. Thus, the thermal coefficient shall be taken as $C_t = 1$.

The roof is considered flat, with low pitch angle. Therefore, the shape coefficient is $\mu_i = 0.8$.

For the characteristic value of snow load on the ground, the highest value expect for the region of Denmark is used. It is $s_k = 1,2 \frac{\text{kN}}{\text{m}^2}$.

Then the snow load on the roof can be calculated:

$$s = 0.8 * 1.2 * 1 * 1.2 = 1,152 \frac{\text{kN}}{\text{m}^2} \quad (3.8)$$

3.5 Wind loads

This section is based on Eurocode EN1991-1-4:2007 [2007].

3.5.1 Quasi-static wind load

First, the quasi-static wind loads on the buildings, when the wind direction is perpendicular to the facade, are calculated. First, the quasi-static wind loads are calculated for building layouts shown in Section 3.1. The width of the buildings is $b = 18\text{ m}$ and depth is $d = 10,8\text{ m}$. Two wind directions are considered separatly, one flowing perpendicular to the width of the buildings and second perpendicular to its depth. Six different heights of building are considered. It will be referred to the buildings' heights by the number of storeys they have, N , as shown in Table 3.3. Also reference height $z_s = 0.6 * h$ for determining the structural factor is outlined in the Table.

Table 3.3: Reference to the heights of the considered buildings

Number of storeys N	Height h [m]	Reference height z_s [m]
1-story	3.6	2.16
2-storeys	7.2	4.32
3-storeys	10.8	6.48
4-storeys	14.4	8.64
5-storeys	18	10.8
10-storeys	36	21.6

The reference height and the dimensions of the buildings are represented on Figure 3.13:

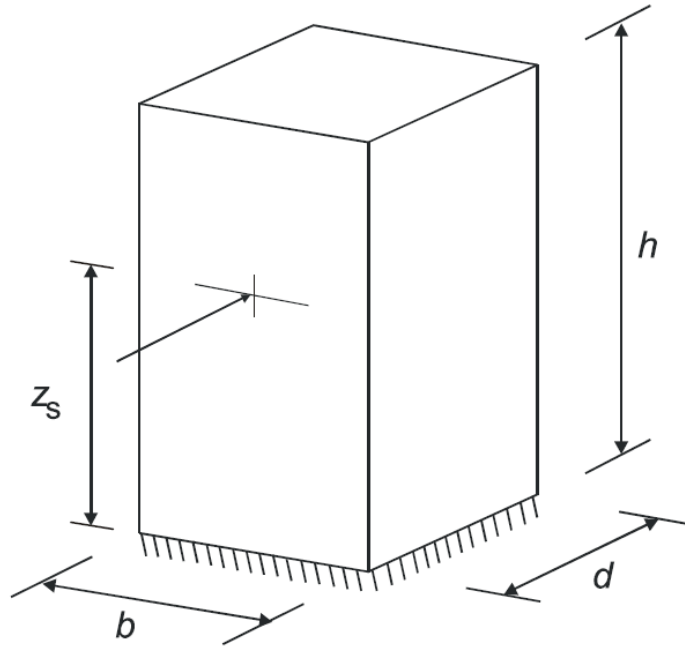


Figure 3.13: Representation of dimensions of the buildings and the reference height

The buildings are considered to be located on the west coast of Denmark in order to account for the worst exposure and wind speed conditions in the region of Denmark. The terrain is considered flat and the building is considered as a permanent structure. Then the basic parameters for the calculation of wind loads are:

Table 3.4: Basic parameters

Symbol	Description	Value
v_{b0}	Fundamental value of basic wind velocity	$27 \frac{\text{m}}{\text{s}}$
c_{dir}	Direction factor	1
c_{season}	Seasonal factor	1
$v_b = v_{b0} * c_{dir} * c_{season}$	Basic wind velocity	$27 \frac{\text{m}}{\text{s}}$
c_0	Orography factor	1
k_p	Peak factor	3.5
ρ	Air density	$1,25 \frac{\text{kg}}{\text{m}^3}$

The buildings are considered to be located in the terrain category I in order to investigate an unfavorable situation of open exposure to wind. This results to:

Symbol	Description	Value
z_0	Roughness length	0.01 m
z_{min}	Minimum height	1 m
$z_{0,II}$	Roughness length (terrain category II)	0.05 m

Then, the terrain factor, k_t , can be determined by:

$$k_t = 0.19 \left(\frac{z_0}{z_{0,II}} \right)^{0.07} = 0.17 \quad (3.9)$$

The upcoming equations are dependent on distance from the ground, z . For this distance the reference height, z_s , is used and while there are six different considered reference heights, the results are stated in Table 3.5.

The roughness factor, c_r , is found by:

$$c_r(z) = k_t \ln \frac{z}{z_0} \quad (3.10)$$

The mean wind speed over a 10 minute period is found by:

$$v_m(z) = c_r(z) c_0 v_b \quad (3.11)$$

The turbulence intensity, $I_v(z)$, is found by:

$$I_v(z) = \frac{1}{c_0 \ln \frac{z}{z_0}} \quad (3.12)$$

The turbulent length scale, $L(z)$, for determining the background factor, B , is found by:

$$L(z) = L_t \left(\frac{z}{z_t} \right)^\alpha \quad (3.13)$$

Where

L_t	Reference length scale, $L_t = 300$ m
z_t	Reference height, $z_t = 200$ m

α is given by:

$$\alpha = 0.67 + 0.05 \ln z_0 = 0.44 \quad (3.14)$$

Table 3.5: Obtained parameters

Number of storeys N	Reference height z_s [m]	$c_r(z_s)$	$v_m(z_s)$	$I_v(z_s)$	$L(z_s)[m]$
1-story	2.16	0.91	24.64	0.186	40.96
2-storeys	4.32	1.03	27.81	0.165	55.55
3-storeys	6.48	1.10	29.67	0.155	66.40
4-storeys	8.64	1.15	30.99	0.148	75.35
5-storeys	10.8	1.19	32.01	0.143	83.12
10-storeys	21.6	1.30	35.19	0.130	112.34

With these, the background factor for a rectangular area, B , is found by Equation 3.15. In this equation, parameter b_{fac} represents width of the facade. When the case of wind blowing in the

direction perpendicular to the wider side of the building is considered, the width of the facade is simply the width of the building $b_{fac} = b = 18$ m. When the case of wind blowing in the direction perpendicular to the slender side of the building is considered, the width of the facade is the depth of the building $b_{fac} = d = 10,8$ m.

$$B^2 = \frac{1}{1 + \frac{3}{2} \sqrt{\left(\frac{b_{fac}}{L(z_s)}\right)^2 + \left(\frac{h}{L(z_s)}\right)^2 + \left(\frac{b_{fac}}{L(z_s)} \frac{h}{L(z_s)}\right)^2}} \quad (3.15)$$

Then the structural factor, $c_s c_d$, can be found:

$$c_s c_d = \frac{1 + 2k_p I_v(z_s) \sqrt{B^2}}{1 + 2k_p I_v(z_s)} \quad (3.16)$$

The wind force, F_w , acting in the direction perpendicular to the facade direction, can be found by:

$$F_w = c_s c_d c_f q_p(z) A_{ref} \quad (3.17)$$

The peak velocity pressure at a given height, $q_p(z)$, can be found by:

$$q_p(z) = [1 + 7I_v(z)] \frac{1}{2} \rho v_m^2(z) \quad (3.18)$$

If the height of the building is lower or equal then the width of the facade, the height at which the peak velocity pressure is calculated is equal to the height of the building, as given by Figure 3.14.

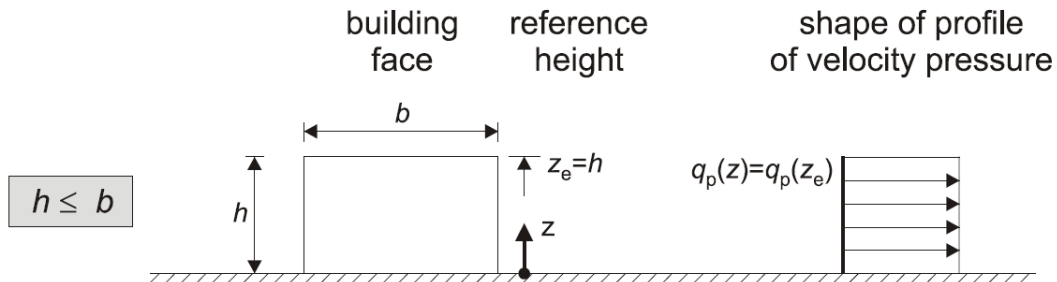


Figure 3.14: Height at which the peak velocity pressure is calculated if $h \leq b$

If the height of the building is higher than the width of the facade but lower than double the width of the facade, the area of the facade is split into two parts. The lower part extending upwards from the ground to a height equal to the width of the facade and the upper part consisting of the remainder. Then the height at which the peak velocity pressure is calculated for each part is represented by Figure 3.15.

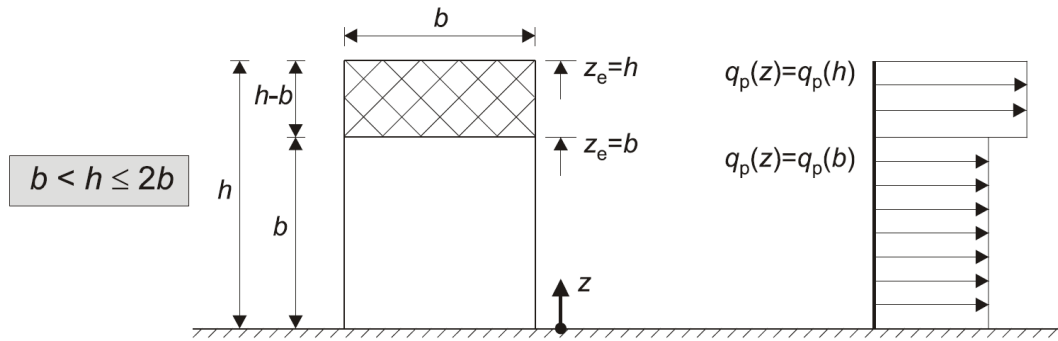


Figure 3.15: Height at which the peak velocity pressure is calculated if $b < h \leq 2b$

In the case of wind direction perpendicular to the slender side of the building, the 10-storeys building is taller than doubled width of the facade. Then the calculation of the peak velocity pressure is governed by Figure 3.16. Only single strip is considered for the middle region.

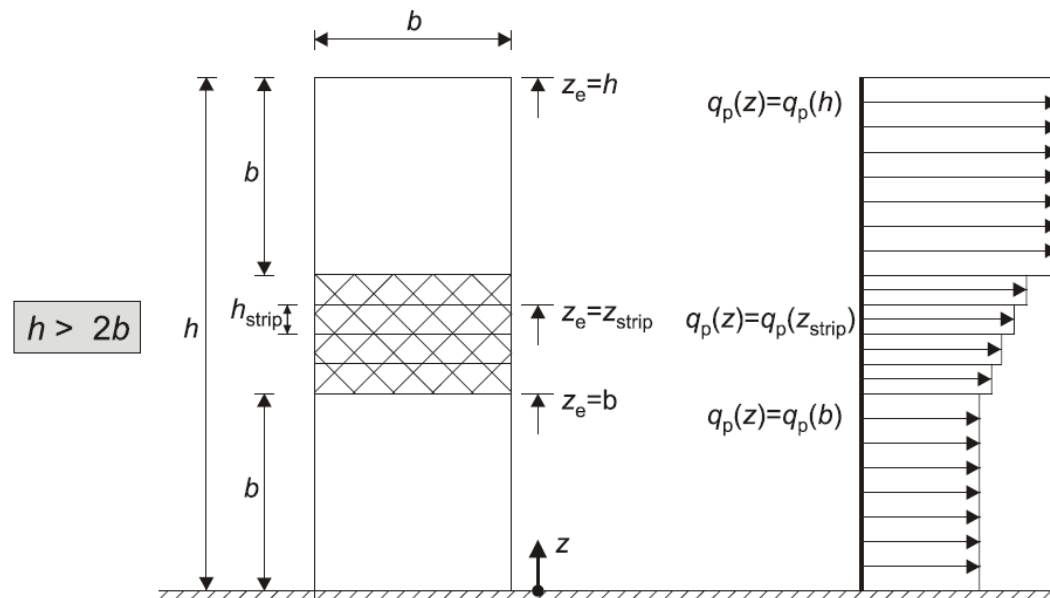


Figure 3.16: Height at which the peak velocity pressure is calculated if $h > 2b$

The force coefficient, c_f , is determined by:

$$c_f = c_{f,0} \psi_r \psi_\lambda \quad (3.19)$$

The force coefficient of rectangular sections, $c_{f,0}$, with sharp corners and without free-end flow is found by the Figure C.1 in Appendix C.

ψ_r is a reduction factor for structures with rounded corners, which is assumed not to be present and is therefore assumed to be equal to 1. ψ_λ is an end-effect factor which can be found via Figure C.2 in Appendix C. The solidity ratio, ϕ , is equal to 1, as there are no openings through the building. Slenderness, λ , is equal to 70, based on Figure C.3 in Appendix C. Then the end-effect factor, ψ_λ , is equal to 0.91.

Now the peak velocity pressures and the wind forces can be calculated. First, the calculation will be conducted for the case of wind perpendicular to the wider side of the building, where the force coefficient of rectangular sections, $c_{f,0}$, is equal to 1.8 and the force coefficient, c_f , is equal to 1.638. Then, calculation of the case of wind perpendicular to the slender side of the building will take place, where $c_{f,0} = 2.35$ and $c_f = 2.139$.

Wind perpendicular to the wider side of the building

Table 3.6: Values of the wind loads induced by wind perpendicular to the wider side of the building

N	B^2	$c_s c_d$	$q_p[\frac{kN}{m^2}]$	$A_{ref}[m^2]$	$F_w[kN]$
1-story	0.597	0.871	0.996	64.8	92.1
2-storeys	0.655	0.898	1.173	129.6	223.6
3-storeys	0.676	0.908	1.283	194.4	370.7
4-storeys	0.683	0.912	1.363	259.2	527.5
5-storeys	0.683	0.913	1.427	324	691.2
10-storeys, lower	0.649	0.907	1.427	324	686.9
10-storeys, upper	0.649	0.907	1.633	324	786.3

Wind perpendicular to the slender side of the building

Table 3.7: Values of the wind loads induced by wind perpendicular to the Slender side of the building

N	B^2	$c_s c_d$	$q_p[\frac{kN}{m^2}]$	$A_{ref}[m^2]$	$F_w[kN]$
1-story	0.705	0.909	0.996	38.88	75.3
2-storeys	0.739	0.925	1.173	77.76	180.4
3-storeys	0.742	0.928	1.283	116.64	296.9
4-storeys, lower	0.735	0.927	1.283	116.64	296.7
4-storeys, upper	0.735	0.927	1.363	38.88	105.1
5-storeys, lower	0.724	0.925	1.283	116.64	296.0
5-storeys, upper	0.724	0.925	1.427	77.76	219.5
10-storeys, lower	0.666	0.912	1.283	116.64	291.8
10-storeys, middle	0.666	0.912	1.525	155.52	462.7
10-storeys, upper	0.666	0.912	1.633	116.64	371.6

Wind acting on a self-standing module

As discussed in section 3.1, the buildings are designed for disassembly and therefore the residential modules need to sustain wind loads also as self-standing structure. In this case the the force coefficient are $c_{f,0} = 2.1$ and $c_f = 1.911$.

Table 3.8: Values of the wind loads induced by wind acting on a self-standing residential module

Type	B^2	$c_s c_d$	$q_p[\frac{kN}{m^2}]$	$A_{ref}[m^2]$	$F_w[kN]$
Self-standing module	0.843	0.954	0.996	12.96	23.53

3.6 Actions during execution

This section is based on Eurocode EN1991-1-4:2005 [2013].

The modules are exposed to special loads due to handling in the construction process. They need to be lifted by their roof when they are loaded on and unloaded from the transportation system and when they are placed at a specific position, either on a foundation or another module.

The lifting mechanism is designed to contain a specialized frame which diminishes lateral actions on the modules. Steel wires are attached to the corners of the frame. These wires can then be connected to top corners of the modules. The same connections used for connecting adjacent modules in a complete building are used for attaching the wires of the lifting mechanism.

The handling load acting on the module is then oriented straight up and its characteristic value is equal to one quarter of the total weight of the module. For the purpose of safe design, a module with all four external walls is considered. Values for self-weight of the elements, expressed in Section 3.2, are used. Then the total weight of the module, $w_{m,t}$, can be calculated as:

$$g_{m,t} = A_s(4g_w + g_r + g_f) + 4G_c \quad (3.20)$$

Where

$w_{m,t}$	Total weight of the module
A_s	Area of the side of the module
w_w	self-weight per m^2 of the wall
w_r	self-weight per m^2 of the roof
w_f	self-weight per m^2 of the floor
w_c	self-weight of the column

Which leads to:

$$g_{m,t} = 3,6 \text{ m} * 3,6 \text{ m} \left(4 * 0,693 \frac{\text{kN}}{\text{m}^2} + 0,969 \frac{\text{kN}}{\text{m}^2} + 1,471 \frac{\text{kN}}{\text{m}^2} \right) + 4 * 1,692 \text{ kN} = 74,32 \text{ kN} \quad (3.21)$$

By dividing the total weight of the module, $w_{m,t}$, by four, we obtain the characteristic value of the handling load:

$$f_{h,c} = \frac{w_{m,t}}{4} = 18,58 \text{ kN} \quad (3.22)$$

Structural design 4

As discussed in Section 1.3.2, corner supported modular system with stiff modules is used as the structural system. Therefore, the main structural elements are the corner supported floors and roofs/ceilings which carry vertical loads and act as diaphragms. These vertical loads are then transferred to columns, which are mostly incorporated in wall elements. Lateral loads are carried by lateral stiffeners, also incorporated in the walls.

4.1 Floor element

Due to use of manufacturing technology described in Section 2.1, the whole floor element will be produced in one piece. The element is 3.6 metres wide, 3.6 metres long and 0.3 metres high. Its top and bottom edges consist of extruded plates with thickness of 3 cm. The infill structure between the plates is shown on Figure 4.1 its detail on Figure 4.2.

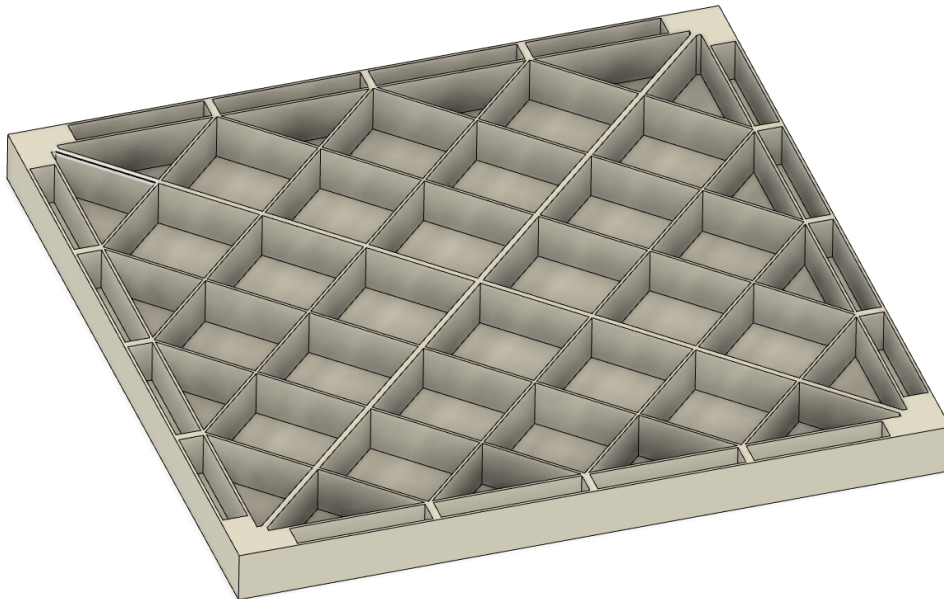


Figure 4.1: Look into the internal structure of the floor element

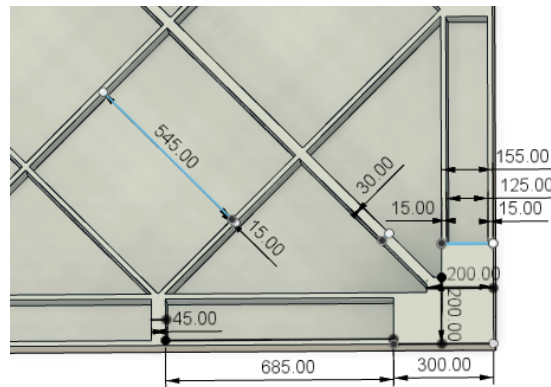


Figure 4.2: Dimensions of the internal structure of the floor element

4.1.1 Serviceability limit state

Due to the character of the POM material, the serviceability limit state (SLS) is considered to be determining, as the material has relatively low stiffness modulus while relatively high strength. Therefore, the structural elements are designed to fulfill SLS and the ultimate limit state is evaluated afterwards.

The maximum deflection of the floor plate is chosen as the SLS design criterion. The maximum global deflection is limited to 12mm. This is rather an arbitrary value as guidelines and standards for the use this type of material in construction are missing.

Load combinations

The uniformly distributed actions on the floor element are the self-weight and the imposed loads. Self-weight of the movable partitions are added to the imposed loads. Characteristic and quasi-permanent load combinations are considered.

The characteristic load combination is considered for short-term effects and is calculated as:

$$q_{ch} = g_f + q_k = 1,141 \frac{\text{kN}}{\text{m}^2} + 2,5 \frac{\text{kN}}{\text{m}^2} = 3,6411 \frac{\text{kN}}{\text{m}^2} \quad (4.1)$$

The quasi-permanent load combination is considered for long-term effects where creep of the material needs to be assessed. The quasi-permanent load combination is calculated as:

$$q_{qp} = g_f + \psi_2 q_k = 1,141 \frac{\text{kN}}{\text{m}^2} + 0.3 * 2,5 \frac{\text{kN}}{\text{m}^2} = 1,891 \frac{\text{kN}}{\text{m}^2} \quad (4.2)$$

Short-term behavior

In the case of the analysis of the short-term behavior, the floor element is considered to be loaded by the characteristic load combination. The load acts on the whole top surface the element. Stiffness of the material is represented by the bending modulus of elasticity, stated in Table 2.1, with value $E_f = 2600 \text{ MPa}$.

The analysis of the floor element is conducted numerically in commercial program Fusion 360. The coordinate system is defined in a way so that y-axis is positive upwards and the x and z-axis follow sides of the element. The boundary conditions are defined with pinned supports positioned at the

bottom of the element at the corners. One support restrict movement in all directions, the adjacent supports allow sliding in x and z direction, respectively. The last support restricts movement only in y-direction. None of the supports restricts rotation.

Figure 4.3 shows short-term displacement of the floor element under characteristic load. The condition of the maximum deflection being smaller than 12mm is satisfied.

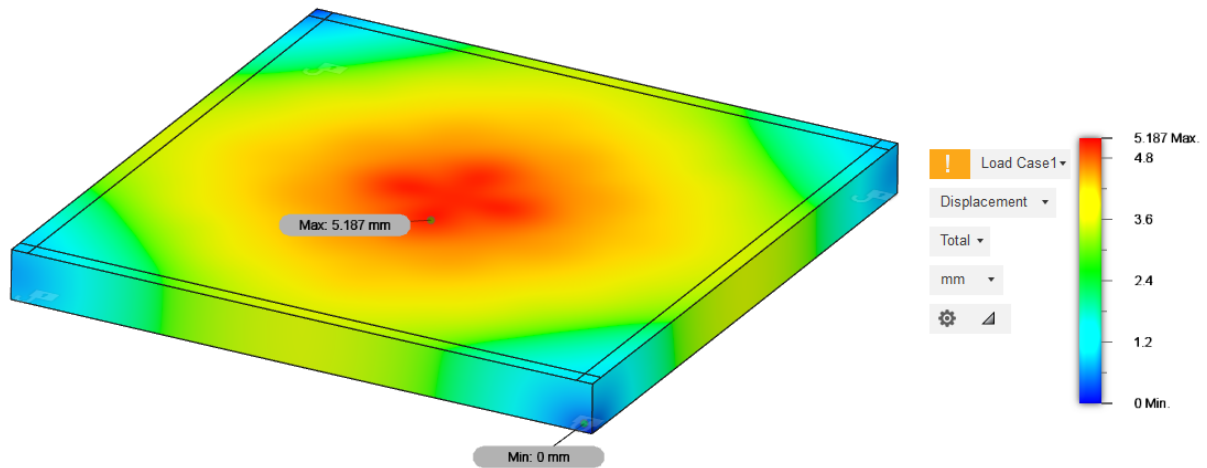


Figure 4.3: Short-term displacement of the floor element

Further, local effects are investigated. Concentrated load $Q_k = 2kN$ is applied on square with side of 50mm, as recommended by EN1991-1-1:2002 [2010]. The load is positioned between the ribs of the infill structure, as illustrated on Figure 4.4. Then the displacement caused by the concentrated load is shown on Figure 4.5. The maximum displacement is 2.7mm, which fulfills the condition.

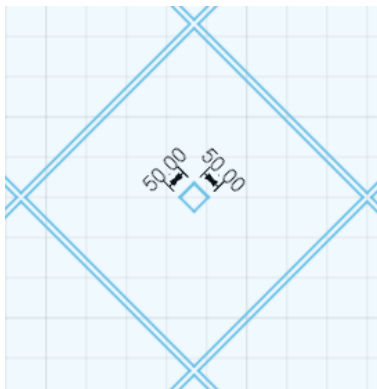


Figure 4.4: Position of the concentrated load Q_k

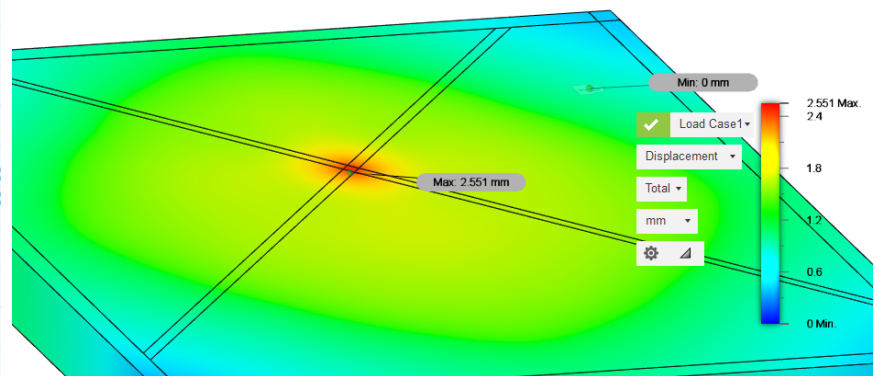


Figure 4.5: Displacement caused by concentrated load Q_k

Long-term behavior

For determination of long-term behavior of the POM material, the apparent stiffness modulus after 40 years of loading, $E_{app,40} = 670MPa$, is used. As described on Section 2.6, $E_{app,40}$ does not represent the actual stiffness of the material. It is just a parameter for determination of strains and displacements of the structural component after 40 years of continual loading.

Boundary conditions and area on which load is applied are defined in the same way as in the case of

short-term analysis. Quasi-permanent load combination is considered. The long-term displacement of the floor element is shown on Figure 4.6. The maximum displacement in y-direction is 11.47mm, which fulfills the criterion.

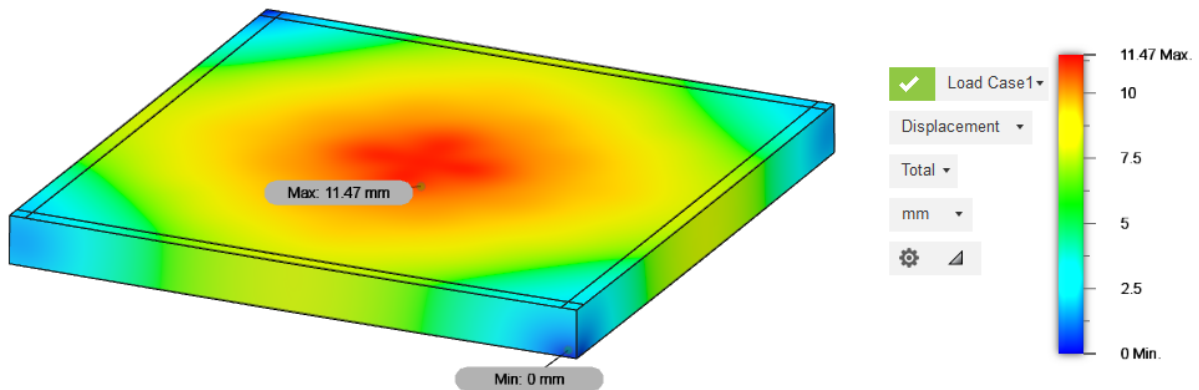


Figure 4.6: Long-term displacement of the floor element

Ultimate limit state

Load combinations

Based on EN1990:2002 [2010], there are two load combinations to consider in the case of ultimate limit state (ULS).

6.10a:

$$\gamma_g g_f + \psi_0 \gamma_q q_k = 1.35 * 1,471 \frac{\text{kN}}{\text{m}^2} + 0.7 * 1.5 * 2,5 \frac{\text{kN}}{\text{m}^2} = 4,61 \frac{\text{kN}}{\text{m}^2} \quad (4.3)$$

6.10b:

$$\xi \gamma_g g_f + \gamma_q q_k = 0.85 * 1.35 * 1,471 \frac{\text{kN}}{\text{m}^2} + 1.5 * 2,5 \frac{\text{kN}}{\text{m}^2} = 5,44 \frac{\text{kN}}{\text{m}^2} \quad (4.4)$$

While load from load combination 6.10b is larger, the load $5,44 \frac{\text{kN}}{\text{m}^2}$ will be used for further calculations of the ultimate limit state. The same material model is used for ULS which was used for SLS short-term behavior. The first principal stresses under ULS are shown on Figure 4.7.

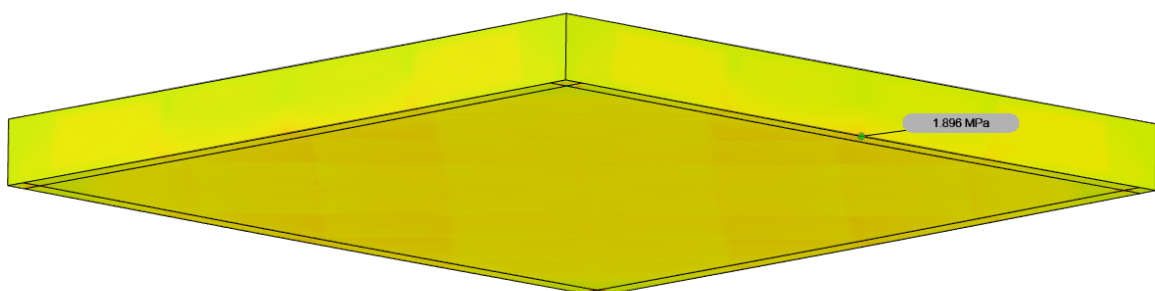


Figure 4.7: First principal stress under ULS

The maximum stress calculated is 1,896 MPa. This is far below the ultimate strength of the material. The design of the floor element is considered to be safe.

Further, local effects are investigated, where the design value of the concentrated load is calculated as:

$$Q_d = \gamma_q Q_k = 1.5 * 2 \text{ kN} = 3 \text{ kN} \quad (4.5)$$

The load is applied in the same way as in the case of investigation of local effects of SLS. The first principal stresses are shown on Figure 4.8. The maximum calculated stress is 7,784 MPa, which is smaller than the ultimate strength of the material.

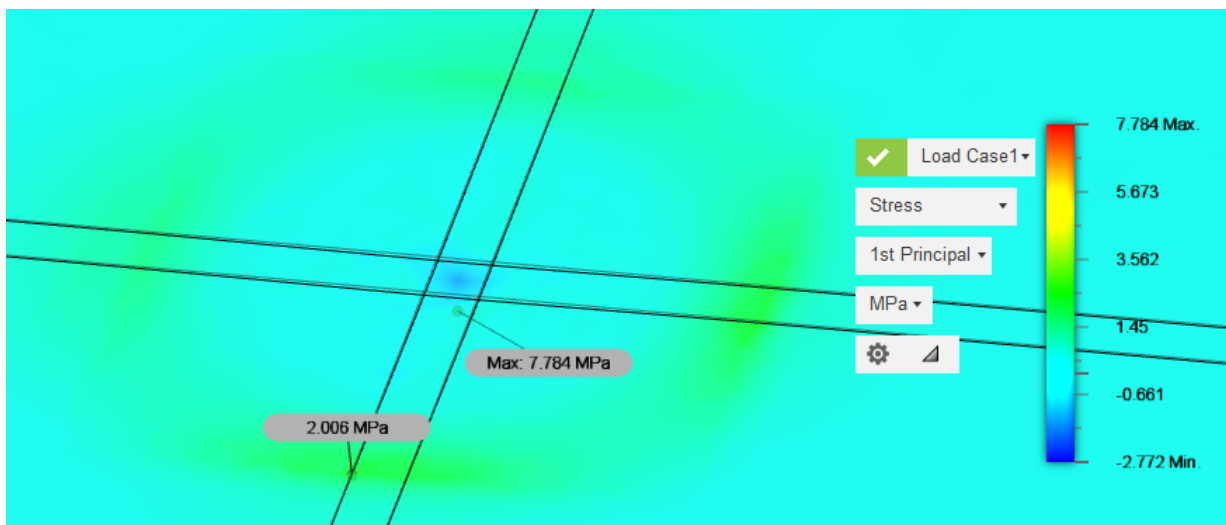


Figure 4.8: First principal stress under local effects of ULS

4.2 Roof element

Roof element is designed in a similar way as the floor element. It has the same overall size: length and width of 3.6 metres and height of 0.3 metres. The roof element also shares the same internal structure as shown on Figure 4.1. However, the thickness of the edge plate of the roof element is 1.5cm, which is half of the thickness in the case of floor element.

4.2.1 Serviceability limit state

Load combination

The actions on the roof element are the self-weight, g_r , and the snow loads, s . The roofs/ceilings of the lower storeys will not in principal experience snow loads. However, the case of the building being disassembled and the modules reused is considered. Therefore, the roof of any module in the structure might eventually experience snow loads in its lifetime.

Then, for analysis of short-term effects, the characteristic load combination is calculated as:

$$q_{ch} = g_r + s = 0.969 \frac{kN}{m^2} + 1.152 \frac{kN}{m^2} = 2.121 \frac{kN}{m^2} \quad (4.6)$$

For long-term effects, the quasi-permanent load combination is calculated as:

$$q_{qp} = g_r + \psi_2 s = 0.969 \frac{kN}{m^2} + 0.3 * 1.152 \frac{kN}{m^2} = 1.315 \frac{kN}{m^2} \quad (4.7)$$

Figures 4.9 and 4.10 then show short-term and long-term displacements of the roof element respectively. In both cases the maximum displacement is smaller than the 12mm limit.

Short-term behavior

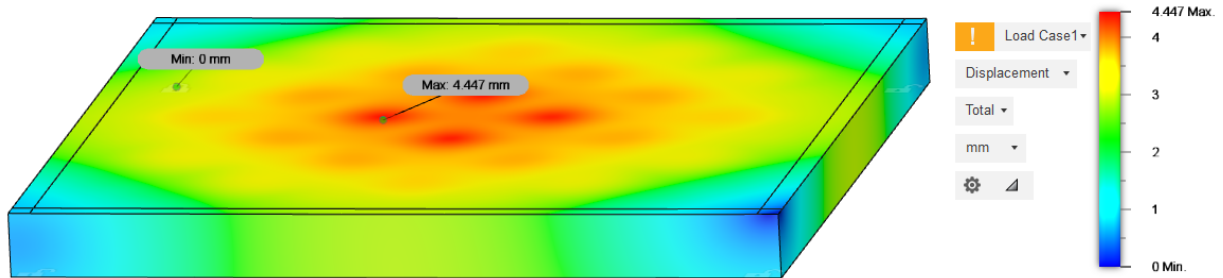


Figure 4.9: Short-term displacement of the roof element

Long-term behavior

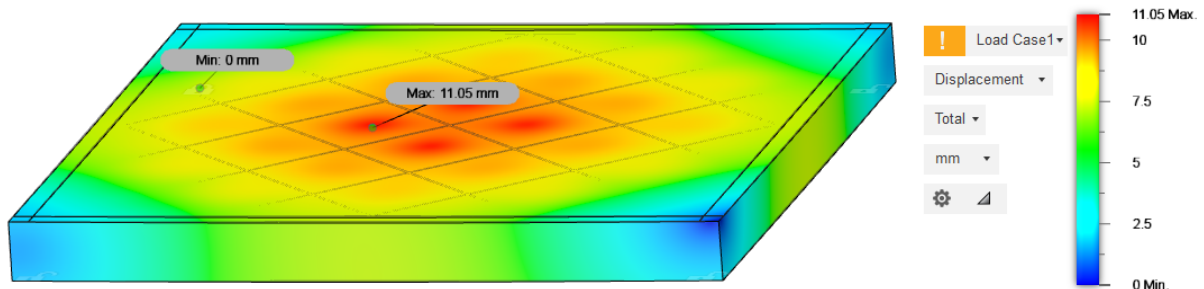


Figure 4.10: Long-term displacement of the roof element

4.2.2 Ultimate limit state

Based on EN1990:2002 [2010], there are two load combinations to consider.

6.10a:

$$\gamma_g g_r + \psi_{0,1} \gamma_q s = 1.35 * 0,969 \frac{kN}{m^2} + 0.7 * 1.5 * 1,152 \frac{kN}{m^2} = 2,52 \frac{kN}{m^2} \quad (4.8)$$

6.10b:

$$\xi \gamma_g g_r + \gamma_q s = 0.85 * 1.35 * 0,969 \frac{kN}{m^2} + 1.5 * 1,152 \frac{kN}{m^2} = 2,84 \frac{kN}{m^2} \quad (4.9)$$

While load from load combination 6.10b is larger, the load $2,84 \frac{kN}{m^2}$ is used for further calculations. The static simulation conducted in Fusion 360 shows the maximal stress to occur in the roof element is 1.54MPa.

4.3 Column

In the case of the buildings under investigation, column is a structural part which is mostly incorporated inside a wall element. However, in some cases it is self-standing and therefore it will be investigated separately.

The loads imposed on the column depend on the amount of storeys which are above the storey in which the column is acting. The loads consist of imposed loads, snow loads and self weight of the structure acting on the column. The specific loads are outlined in table 4.1. It is considered that the column carries one quarter of the module above. Case in which two walls meet above the column is considered.

Table 4.1: Loads acting on the column

Load origin	Calculation	Action on column [kN]
roof s.w.	$0,969 \frac{\text{kN}}{\text{m}^2} * 1,8 \text{ m} * 1,8 \text{ m}$	3.14
floor s.w.	$1,141 \frac{\text{kN}}{\text{m}^2} * 1,8 \text{ m} * 1,8 \text{ m}$	4.48
column s.w.	-	1.692
2 walls s.w.	$2 * 0,693 \frac{\text{kN}}{\text{m}^2} * 1,6 \text{ m} * 3 \text{ m}$	6.65
imposed load	$2,5 \frac{\text{kN}}{\text{m}^2} * 1,8 \text{ m} * 1,8 \text{ m}$	8.1
snow load	$1,152 \frac{\text{kN}}{\text{m}^2} * 1,8 \text{ m} * 1,8 \text{ m}$	3.73

Loads caused by self-weights of the structural elements are summed up into a single value representing self-weight of a quarter of the module, $G_{ST,c}$:

$$G_{ST,c} = 3.14kN + 4.48kN + 1.692kN + 6.65kN = 15.96kN \quad (4.10)$$

The self-weight of the roof is labeled separately as $G_{R,c} = 3.14kN$ to take into account the weight of the roof located in the same module in which the column under investigation is located. Further, imposed loads are labeled as $Q_{in,c} = 8.1kN$ and snow loads as $Q_{s,c} = 3.73kN$.

Then for all the considered number of storeys, n , the characteristic load combination, Q_{ch} , is calculated with Equation 4.11, quasi-permanent load combination, Q_{qp} , with Equation 4.12. As the permanent loads are dominant, only load combination 6.10a, $Q_{6.10a}$, is considered in the ULS analysis, calculated with Equation 4.13. Imposed loads, $Q_{in,c}$, are multiplied by reduction factor, α_n , described in Section 3.3.

$$Q_{ch} = G_{R,c} + (n - 1)G_{ST,c} + (n - 1)\alpha_n Q_{in,c} + Q_{s,c} \quad (4.11)$$

$$Q_{qp} = G_{R,c} + (n - 1)G_{ST,c} + \psi_2((n - 1)\alpha_n Q_{in,c} + Q_{s,c}) \quad (4.12)$$

$$Q_{6.10a} = \gamma_g(G_{R,c} + (n - 1)G_{ST,c}) + \psi_0\gamma_q(\alpha_n(n - 1)Q_{in,c} + Q_{s,c}) \quad (4.13)$$

Load combinations for all the considered number storeys, n , are shown in Table 4.2.

Table 4.2: Load combinations acting on the columns

Number of storeys, n	Q_{ch} [kN]	Q_{qp} [kN]	$Q_{6.10a}$ [kN]
1	6.87	4.26	8.16
2	30.93	22.65	38.21
3	53.37	40.55	66.56
4	75.41	58.34	94.48
5	97.28	76.07	122.24
10	205.91	164.52	260.24

In order to carry the loads expressed in Table 4.2, four types of columns are designed. Their cross-sections are shown on Figure 4.11. The thickness of the walls is determined by the limitations of the manufacturing technology, more specifically by the thickness of the edge plate and size of the bead. The thickness of the edge plate is 1cm. The thicknesses of the walls of the columns are then multiplications of the size of the bead added to the thickness of the edge plate.

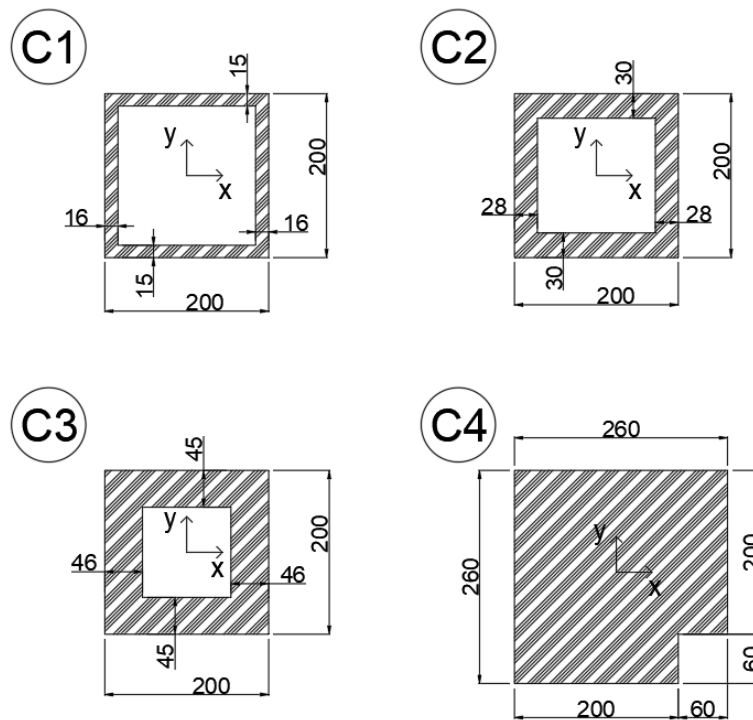


Figure 4.11: Cross-sections of the columns

An important parameter of the cross-sections is the critical buckling force, P_{cr} . The column is considered to simply supported and therefore P_{cr} can be calculated analytically with Equation 4.14.

$$P_{cr} = \frac{\pi^2 E_f I_{min}}{l^2} \quad (4.14)$$

Where

P_{cr}	Critical buckling force
E_f	Modulus of elasticity (bending)
I_{min}	Minimal cross-sectional moment of inertia
l	Length of the column

Further, the critical stress, σ_{cr} , at which buckling occurs can be calculated with Equation 4.15.

$$\sigma_{cr} = \frac{P_{cr}}{A} \quad (4.15)$$

Where

σ_{cr}	Critical buckling stress
A	Cross-sectional area

The cross-sectional parameters of the columns represented on Figure 4.11 are summarized in Table 4.3.

Table 4.3: Cross-sectional parameters of the columns

Column type	$A [m^2]$	$I_y [m^4]$	$I_x [m^4]$	$I_{min} [m^4]$	$P_{cr} [kN]$	$\sigma_{cr} [MPa]$
C1	0.01144	$6.46 * 10^{-5}$	$6.62 * 10^{-5}$	$6.46 * 10^{-5}$	184.05	16.09
C2	0.01984	$10.04 * 10^{-5}$	$9.85 * 10^{-5}$	$9.85 * 10^{-5}$	280.85	14.16
C3	0.0283	$12.14 * 10^{-5}$	$12.18 * 10^{-5}$	$12.14 * 10^{-5}$	346	12.23
C4	0.064	$34.17 * 10^{-5}$	$34.17 * 10^{-5}$	$30.37 * 10^{-5}$	865.86	13.53

These values of critical buckling forces were also compared to numerical buckling analysis conducted numerically in Fusion 360. The analytical values correspond to the numerical results related to the first buckling mode. Numerical analysis also proves, that local buckling occurs at higher forces than global buckling of the column.

4.3.1 Serviceability limit state

The maximum displacement of 12mm is chosen as the serviceability limit state criterion for the design of the column. First, stress in the material caused by homogeneous compressive force is calculated simply with Equation 4.16. In the case of the analysis of short-term behavior, characteristic values of load combinations acting on the column, Q_{ch} , from Table 4.2 are used as loads in Equation 4.16. In the case of long-term analysis, quasi-permanent load combination, Q_{qp} , is acting.

$$\sigma = \frac{Q}{A} \quad (4.16)$$

The strain in the material is then calculated with Equation 4.17. In this Equation, $E_c = 2300MPa$ presented on Table 2.1 is used for the short-term analysis and $E_{app,40} = 670MPa$ expressed in Section 2.6 is used for long-term analysis.

$$\epsilon = \frac{\sigma}{E} \quad (4.17)$$

Finally, the deformation of the column or the change of its length, δ , is calculated with Equation 4.18, where l_0 represents initial length of the column.

$$\delta = l_0 \epsilon \quad (4.18)$$

The types of columns used for buildings with specific number of storeys and the corresponding stresses, strains and deformations are shown in Tables 4.4 and 4.5 correspondingly.

Short-term behavior

Table 4.4: Short-term behavior of the columns

Number of storeys	Column type	Q_{ch} [kN]	σ [MPa]	σ_{cr} [MPa]	ϵ [%]	δ [mm]
1	C1	6.87	0.601	16.09	0.026	0.78
2	C1	30.93	2.704	16.09	0.118	3.53
3	C2	53.37	2.690	14.16	0.117	3.51
4	C3	75.41	2.665	12.23	0.116	3.55
5	C3	97.28	3.437	12.23	0.149	4.48
10	C4	205.91	3.217	13.53	0.140	4.20

Long-term behavior

Table 4.5: Long-term behavior of the columns

Number of storeys	Column type	Q_{qp} [kN]	σ [MPa]	σ_{cr} [MPa]	ϵ [%]	δ [mm]
1	C1	4.26	0.372	16.09	0.056	1.67
2	C1	22.65	1.980	16.09	0.295	8.86
3	C2	40.55	2.044	14.16	0.305	9.15
4	C3	58.34	2.061	12.23	0.308	9.23
5	C3	76.07	2.688	12.23	0.401	12.0
10	C4	164.52	2.571	13.53	0.384	11.5

4.3.2 Ultimate limit state

Equation 4.16 is used for calculation of the stresses in the columns under ultimate load combination, $Q_{6.10a}$. The results are shown in Table 4.6. It is clear that the stresses in the columns are much lower than the critical stresses.

Table 4.6: Stresses in the columns under ultimate load combination

Number of storeys	Column type	$Q_{6.10a}$ [kN]	σ [MPa]	σ_{cr} [MPa]
1	C1	8.16	0.713	16.09
2	C1	38.21	3.340	16.09
3	C2	66.56	3.355	14.16
4	C3	94.48	3.339	12.23
5	C3	122.24	4.319	12.23
10	C4	260.24	4.066	13.53

4.4 Lateral stiffener

As explained in Section 1.3.2 the structural system used for the buildings analysed in the scope of this project is the corner supported modular system with stiff modules. The stiff modules are designed to carry lateral loads imposed on the buildings. As discussed in Section 3.1, the residential modules are designed also for the case of being used as self-standing structures. Therefore, the residential modules have to be inherently stiff and thus they are the stiff modules of the buildings.

The walls of the residential modules incorporate lateral stiffeners, which provide them with the necessary lateral stiffness. Each residential module contain three lateral stiffeners. Their placement in the structure is shown on Figure 4.12.

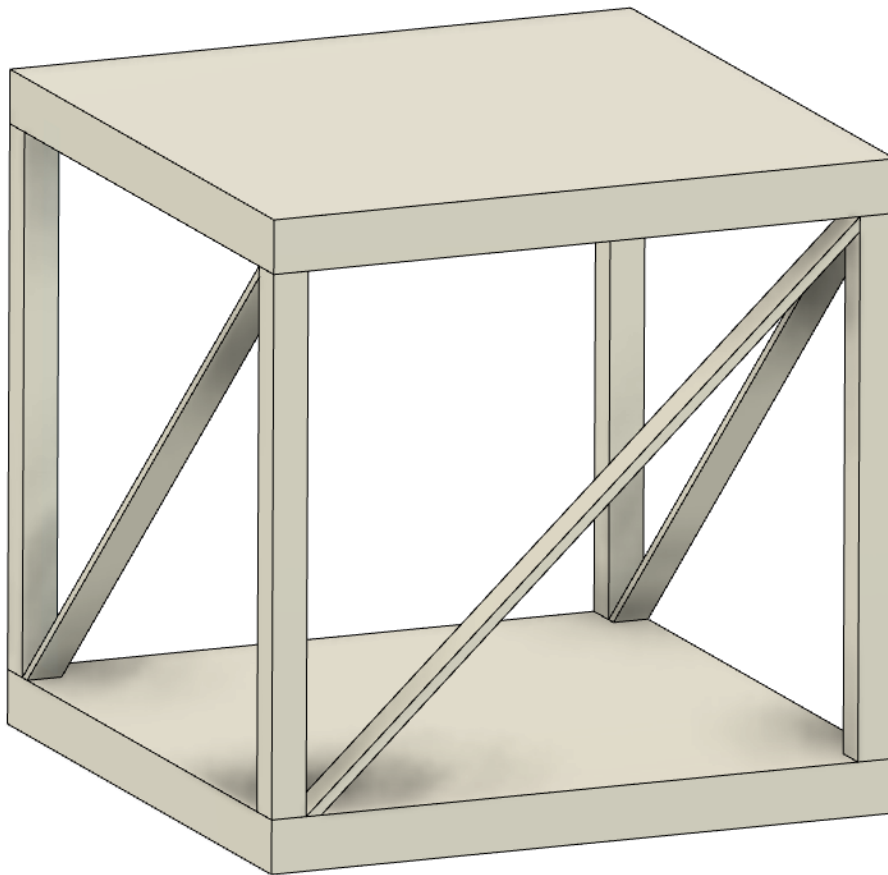


Figure 4.12: Placement of the lateral stiffeners in residential module

As shown in Table 3.8 the wind load acting on each side of the self-standing module is $F_w = 23.53kN$. When this load is applied in a way so only the single lateral stiffener is acting, then half of the load is considered to be absorbed by the foundations and the other half is acting on the top of the module. Such loading of the stiffener is represented on Figure 4.13. The connections between all the elements are considered as hinges. Therefore the normal force in the stiffener can be calculated with Equation 4.19.

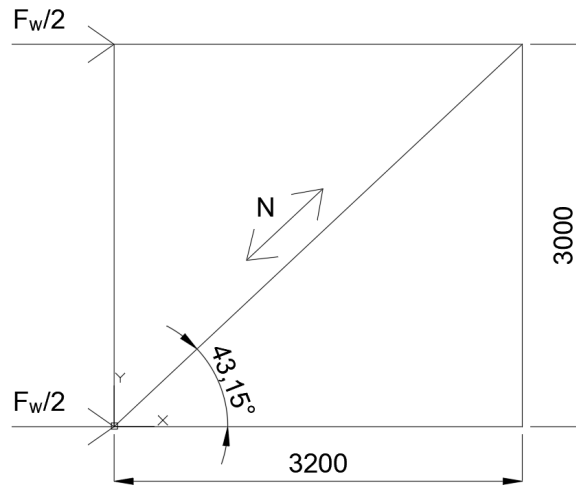


Figure 4.13: Conceptual loading of the stiffener

$$N = \frac{F_h}{\cos 43.15^\circ} \quad (4.19)$$

Where

$$\begin{array}{l|l} N & \text{Normal force in the stiffener} \\ F_h & \text{Horizontal force acting on the top of the stiffener} \end{array}$$

In the case of the single stiffener under consideration, the horizontal force, F_h , is equal to half of $F_w = 23.53kN$. Then the normal force is $N = 16.13kN$. Lets consider that a bracing rod made of steel S355 with diameter of 10mm was used to carry this load. The stress in the stiffener would be $\sigma = 205.46MPa$, calculated with Equation 4.20. The strain in the stiffener would be $\epsilon = 0.098\%$, calculated with Equation 4.21. The elongation of the stiffener would be $\delta_l = 4.29mm$, calculated with Equation 4.22. And the lateral displacement of the top of the frame on Figure 4.13 would be $u = 3.13mm$, calculated with Equation 4.23. Based on this calculation, the lateral displacement allowed by a lateral stiffener will be limited to 4mm.

$$\sigma = \frac{N}{A} \quad (4.20)$$

Where

$$\begin{array}{l|l} \sigma & \text{Normal stress in the stiffener} \\ A & \text{Cross-sectional area of the stiffener} \end{array}$$

$$\epsilon = \frac{\sigma}{E} \quad (4.21)$$

Where

$$\begin{array}{l|l} \epsilon & \text{Strain in the stiffener} \\ E & \text{Young's modulus of the material of the stiffener} \end{array}$$

$$\delta_l = l_0 \epsilon \quad (4.22)$$

Where

δ_l | Elongation of the stiffener
 l_0 | Initial length of the stiffener, $l_0 = 4.3863\text{m}$

$$u = \delta_l \cos 43.15^\circ \quad (4.23)$$

Where

u | Lateral displacement of the stiffened frame

Six designs are used as the lateral stiffeners, shown on Figure 4.14. The designs L1 to L4 use POM exclusively. In the case of the designs L5 and L6 a channel is created between a doubled POM stiffener and steel rods are inserted inside of the channel, one rod in the case of L5 and two in the case of L6. Nine diameters of the steel rods are used: 6mm, 8mm, 10mm, 12mm, 16mm, 20mm, 24mm, 27mm and 30mm. Steel S355 is used.

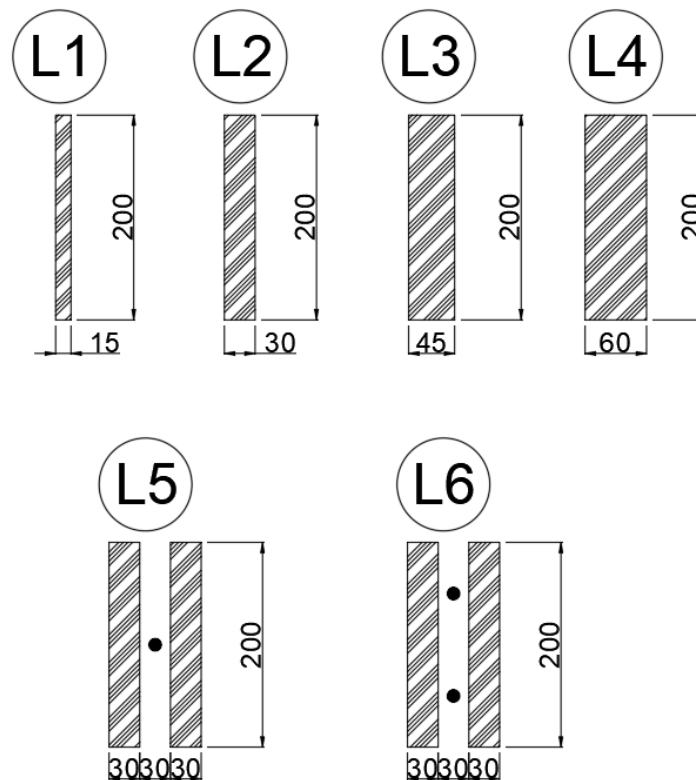


Figure 4.14: Cross-sections of the lateral stiffeners

In the case of the self-standing module, design L2 is suitable for the single lateral stiffener and designs L1 are suitable for the pair of the parallel stiffeners.

Inside of the buildings under consideration the lateral stiffeners are placed in planes represented on Figure 4.15. The red lines represent planes along the wider side of the buildings. Side view of these stiffeners is presented on Figure 4.16. The middle stiffener is missing in the case of the plane which is crossing the staircase. Therefore, there are 9 stiffeners in each storey along the longer side of the buildings.

Blue lines represent planes along the slender side of the buildings, whose side view is shown on Figure 4.17. There are 10 such planes and two stiffeners in each, which leads to 20 lateral stiffeners along the slender side of the buildings.

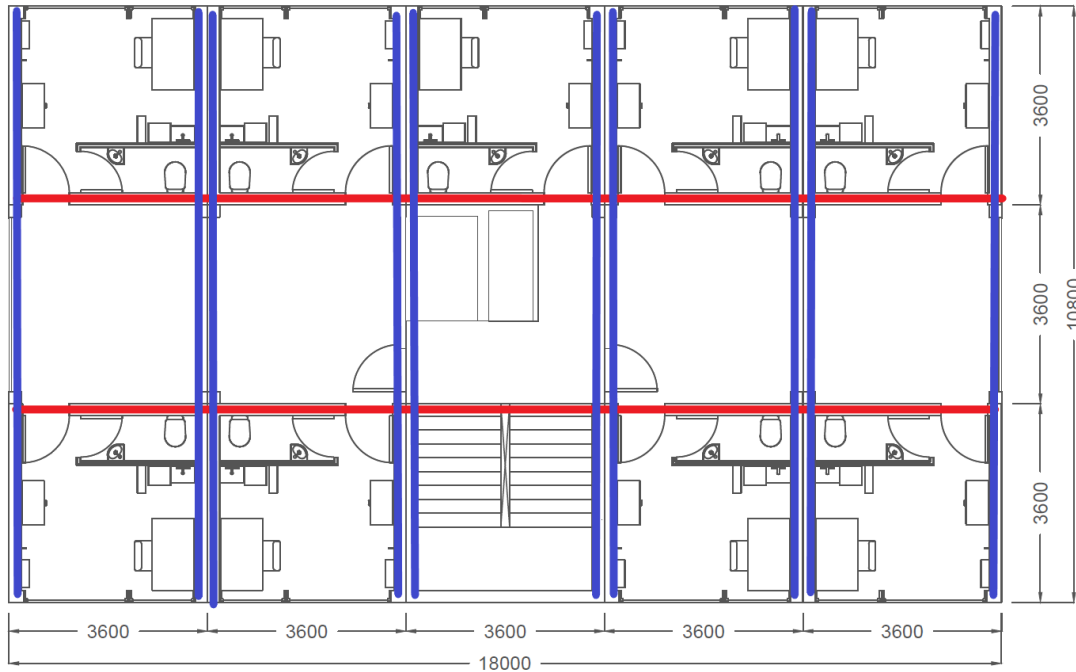


Figure 4.15: Planes of placement of lateral stiffeners

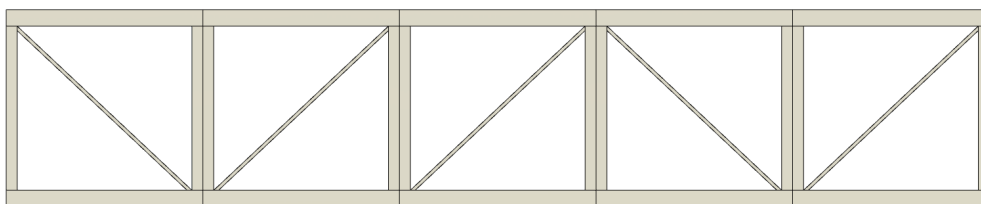


Figure 4.16: Placement of lateral stiffeners through the wider side of the buildings

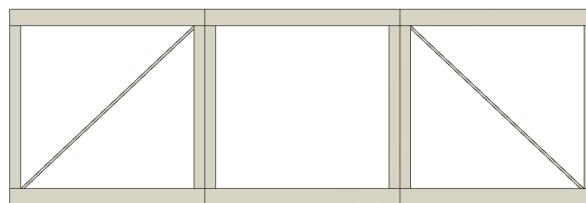


Figure 4.17: Placement of lateral stiffeners through the slender side of the buildings

The designs L1 to L4 on Figure 4.14 are capable to carry loads both in tension and compression as

the walls' edge plates are restricting them from buckling. However, steel bracing rods of designs L5 and L6 and only capable to carry tension forces. Therefore, along the slender sides of the buildings the steel bracing rods are considered to act only in 10 lateral stiffeners. Along the wider sides of the buildings the steel bracing rods are considered to act only in 4 lateral stiffeners, as the middle stiffener on Figure 4.16 is designed without the steel rods due to symmetry.

Then the designs of the stiffeners incorporated in the buildings is conducted through the following procedure:

- The horizontal loads acting on the top of each storey are calculated as sum of all the wind forces, from Table 3.6 and 3.7, acting on half of the storey under consideration and on all the storeys above this storey. An example of this process is represented by Figure 4.18.
- Equation 4.19 is used to calculate total normal force. In this process, all the stiffeners are mathematically modeled as a single stiffener.
- First design on Figure 4.14 is assigned to all the stiffeners. Cross-sectional area of all the stiffeners as summed up and used in Equation 4.20.
- Equations 4.21, 4.22 and 4.23 are used to calculate total lateral displacement of the floor.
- If the displacement is larger then the limit of 4mm, next design on Figure 4.18 is used. Area of the steel rods is taken into account as an equivalent area of the POM material, expressed with Equation 4.24. Only the steel bracing rods acting in tension are taken into account.

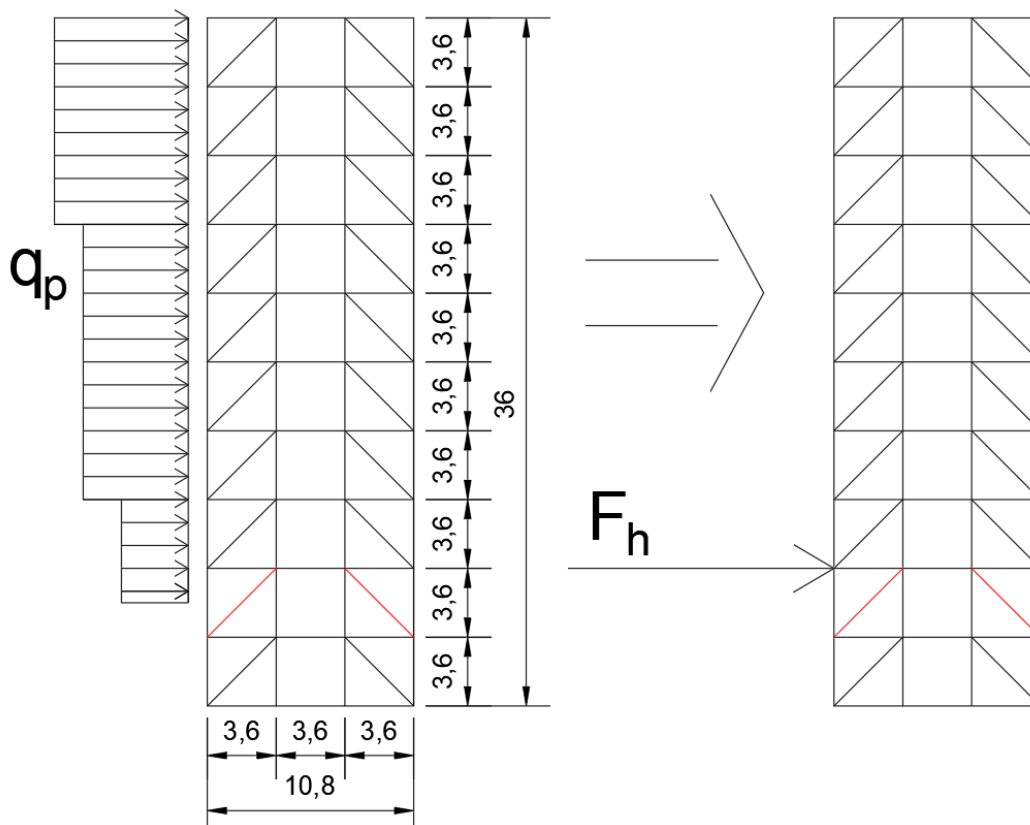


Figure 4.18: Example of the loads acting on stiffeners of the second floor of 10 storey building

$$A_{s,eq} = A_s \frac{E_{steel}}{E_{POM,t}} \quad (4.24)$$

Where

$A_{s,eq}$	Equivalent area of the steel bracing rods
A_s	Area of the steel bracing rods
E_{steel}	Young's modulus of the steel S355, $E_{steel} = 210\text{GPa}$
$E_{POM,t}$	Young's modulus of POM in tension, $E_{POM,t} = 2.8\text{GPa}$

This process is applied to all the storeys of all the buildings under consideration for wind loads perpendicular to the wider and the slender sides of the buildings.

Table 4.7: Stiffeners of all the buildings under consideration

		Along wider side			Along slender side		
Building	Storey	F_h [kN]	stiffener	bracing rod	F_h [kN]	stiffener	bracing rod
1 storey	1st	37.646	L1	-	46.058	L1	-
2 storey	2nd	45.105	L1	-	55.891	L1	-
	1st	135.316	L2	-	167.674	L2	-
3 storey	3rd	49.481	L1	-	61.782	L1	-
	2nd	148.444	L3	-	185.345	L2	-
	1st	247.406	L4	-	308.908	L3	-
4 storey	4th	52.542	L1	-	65.942	L1	-
	3rd	154.531	L3	-	197.827	L2	-
	2nd	253.424	L4	-	329.711	L3	-
	1st	352.317	L5	ø12mm	461.595	L4	-
5 storey	5th	54.880	L1	-	69.126	L1	-
	4th	164.641	L3	-	207.379	L2	-
	3rd	268.859	L4	-	345.632	L3	-
	2nd	367.535	L5	ø16mm	483.885	L4	-
	1st	466.211	L5	ø20mm	622.138	L5	ø6mm
10 storey	10th	61.929	L1	-	78.631	L1	-
	9th	185.786	L3	-	235.892	L2	-
	8th	309.643	L5	ø8mm	393.154	L3	-
	7th	429.412	L5	ø16mm	550.415	L4	-
	6th	545.092	L5	ø24mm	707.677	L5	ø8mm
	5th	660.773	L5	ø27mm	854.998	L5	ø16mm
	4th	776.453	L5	ø30mm	992.378	L5	ø16mm
	3rd	882.930	L6	2X ø24mm	1129.759	L5	ø20mm
	2nd	980.202	L6	2X ø27mm	1267.140	L5	ø24mm
	1st	1077.474	L6	2X ø27mm	1404.520	L5	ø24mm

Structural connections 5

This chapter describes design and analysis of the structural connections used in the buildings.

5.1 Intra-module connections

Intra-module connections are connecting structural elements within the modules. Steel bolts and nuts of class 4.6 are used. According to Troughton [2008], use of screws and retaining nuts provide a simple and convenient method to assemble plastic parts. This method allows multiple reassembles which is desirable as it enables reuse and recycling of the structural elements. The assembly method requires attention to the following:

- The joint area should be assembled in a way which eliminates any space between the two surfaces being assembled.
- A washer should be used to distribute the high torque loading over a greater surface area.

5.1.1 Type 1 connection

Type 1 connection is designed to join floor element, column and lateral stiffeners without steel bracing rods.

Figures 5.1 and 5.2 show side-view sections of the Type 1 connection which is linking roof, column and lateral stiffeners L1 to L4. Figure 5.2 shows the lateral stiffener and the column which are incorporated in a common wall. Figure 5.2 shows the lateral stiffener which is incorporated in a separate wall. Figure 5.3 shows top-view section of the connection and Figure 5.4 view from the bottom.

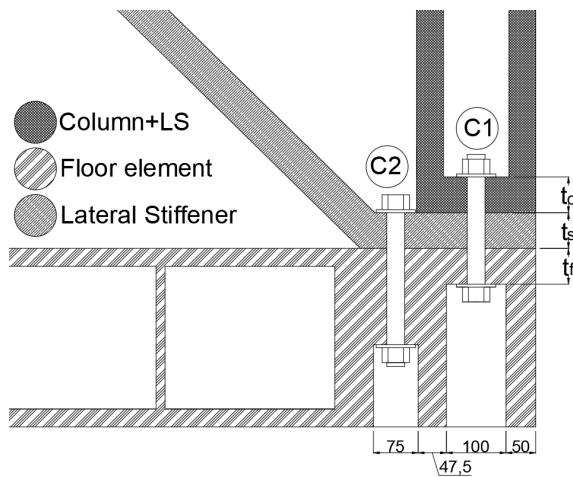


Figure 5.1: A-A' side-view section of the type 1 connection

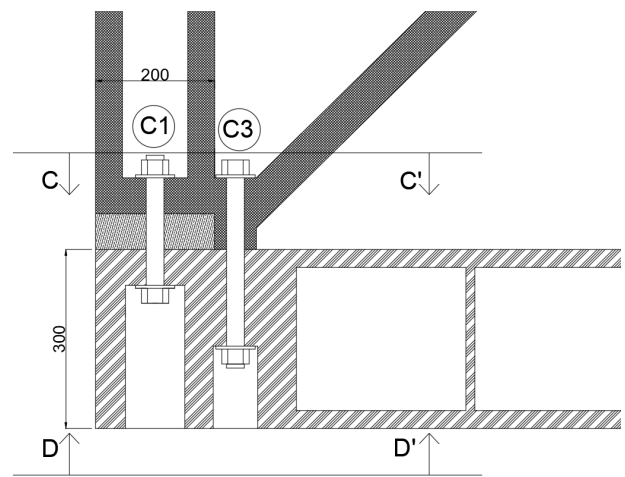


Figure 5.2: B-B' side-view section of the type 1 connection

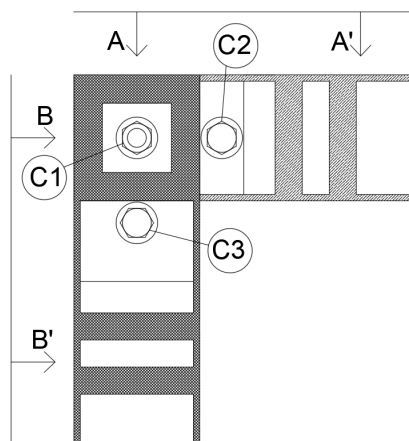


Figure 5.3: C-C' top-view section of the type 1 connection

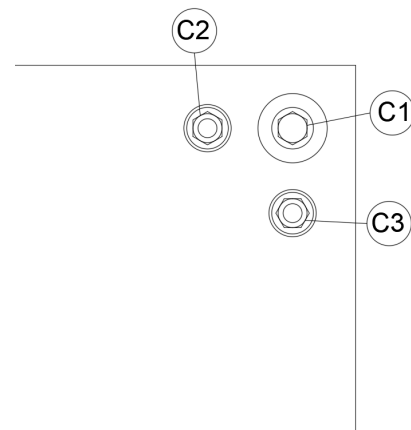


Figure 5.4: Bottom-view of the type 1 connection

Only three bolts join all the elements: C1, C2 and C3. These bolts are designed to carry tension and shear forces. Tension forces originate from loads during execution, Section 3.6, and wind loads, Section 3.5. Shear forces are caused by wind loads.

The bolt C1 have to carry the handling load, $F_{H,c} = 18.58$, calculated in Section 3.6. This load is multiplied by force factor, $\gamma_f = 1.5$, to take into account dynamic effects which might occur during execution. Then the horizontal load that needs to be carried by bolt is C1 is:

$$F_{H,d} = F_{H,c} \gamma_f = 18.58 \text{ kN} * 1.5 = 27.87 \text{ kN} \quad (5.1)$$

Based on Eurocode EN1991-1-8:1992 [2005], the tension resistance of the bolt can be calculated with Equation 5.2.

$$F_{t,Rd} = \frac{k_2 f_{ub} A_s}{\gamma_{M2}} \quad (5.2)$$

Where

$F_{t,Rd}$	Tension resistance of the bolt
k_2	Reduction factor $k_2 = 0.9$
f_{ub}	Ultimate tensile strength of the bolt, $f_{ub} = 400\text{MPa}$ for class 4.6
A_s	Tensile stress area of the bolt
γ_{M2}	Partial safety factor for joints, $\gamma_{M2} = 1.25$

We can rearrange Equation 5.2 to express the required tensile stress area when force $F_{H,d}$ is applied:

$$A_{s,req} = \frac{F_{t,Rd}\gamma_{M2}}{k_2 f_{u,b}} = \frac{27.87\text{kN} * 1.25}{0.9 * 400\text{MPa}} = 96.77\text{mm}^2 \quad (5.3)$$

A bolt with satisfactory tensile stress area is the bolt M14. Its tensile stress area is $A_s = 115\text{mm}^2$.

Further, punching shear resistance needs to be calculated to verify if the head of the bolt does not puncture the plastic material. It can be calculated with Equation 5.4.

$$B_{p,Rd} = \frac{0.6\pi d_m t_p f_u}{\gamma_{M2}} \quad (5.4)$$

Where

$B_{p,Rd}$	Punching shear resistance
d_m	The mean of the across points and across flats dimensions of the bolt head or the nut, whichever is smaller
t_p	Thickness of the plate under bolt head or nut
f_u	Ultimate strength of the material which is joined by the bolt
γ_{M2}	Partial safety factor for joints, $\gamma_{M2} = 1.25$

By rearranging Equation 5.4 the required thickness of the plate for different types of bolts can be calculated. For bolt M14, $d_m = 22.2\text{mm}$. $f_u = 43\text{MPa}$ is used for the ultimate strength of the POM material.

$$t_{p,req} = \frac{F_{H,d}\gamma_{M2}}{0.6\pi d_m f_u} = \frac{27.87\text{kN} * 1.25}{0.6 * \pi * 0.0222\text{m} * 43\text{MPa}} = 0.194\text{m} \quad (5.5)$$

Thus, plate of thickness 2cm is required if bolt M14 is used to carry the loads during execution. This is required for thickness of plate at the bottom of the column, t_c , and the plate at the top of the floor, t_f , described on Figure 5.1.

By reversing the process described by Equations 4.20 to 4.23, the maximal normal force, N_{max} , experienced by a given type of the lateral stiffener can be calculated. For that, vertical, $F_{v,max}$, and horizontal, $F_{h,max}$, components can be found. By multiplying those forces with force factor $\gamma_f = 1.5$, design values, $F_{v,d}$ and $F_{h,d}$, are obtained. These forces are stated in Table 5.1.

Table 5.1: Maximal forces acting on the lateral stiffeners

Lateral stiffener	N_{max} [kN]	$F_{v,max}$ [kN]	$F_{v,d}$ [kN]	$F_{h,max}$ [kN]	$F_{h,d}$ [kN]
L1	10.5	7.18	10.77	7.66	11.49
L2	21	14.36	21.54	15.32	22.98
L3	31.5	21.54	32.31	22.98	34.47
L4	42	28.72	43.08	30.64	45.96

Design values of the vertical forces are then applied in Equation 5.3 to obtain the required tensile stress areas of bolt C2 and C3. Then the satisfactory types of the bolts can be determined. That information is further used to calculate the required thickness of the material connected by the bolts, with use of Equation 5.5. The results are presented in Table 5.5.

Table 5.2: Tension parameters of bolts C2, C3

Lateral stiffener	$F_{v,d}$ [kN]	$A_{s,req}$ [mm ²]	Bolt type	$t_{p,req}$ [mm]
L1	10.77	37.40	M10	14.7
L2	21.54	74.79	M12	26.2
L3	32.31	112.19	M14	33.7
L4	43.08	149.58	M16	39.2

Further, bolts C1,C2 and C3 must be able to carry shear forces caused by horizontal loads induced by lateral stiffeners. Shear resistance of the bolts is calculated with Equation 5.6.

$$F_{v,Rd} = \frac{\alpha_v f_{ub} A}{\gamma_{M2}} \quad (5.6)$$

Where

$F_{v,Rd}$	Shear resistance per shear plane
α_v	Reduction factor, $\alpha_v = 0.6$, for the case of the shear plane passing through the unthreaded portion of the bolt
f_{ub}	Ultimate strength of the bolt, $f_{ub} = 400\text{MPa}$ for bolt class 4.6
A	The gross cross-section of the bolt
γ_{M2}	Partial safety factor for joints, $\gamma_{M2} = 1.25$

From Equation 5.6, the required gross cross-section area of the bolt can be expressed, as shown in Equation 5.7. Design values of the vertical force from Table 5.1 are used. The values of required gross cross-section area, A_{req} , and the necessary types of bolts are shown in Table 5.3. There are always two bolts acting.

$$A_{req} = \frac{F_{v,d} \gamma_{M2}}{\alpha_v f_{ub}} \quad (5.7)$$

Table 5.3: Shear resistance

Lateral stiffener	$F_{h,d}$ [kN]	A_{req} [mm ²]	Bolt type
L1	11.49	59.84	2X M8
L2	22.98	119.69	2X M10
L3	34.47	179.53	2X M12
L4	45.96	239.38	2X M14

Finally the bearing resistance of the joined material needs to be tested. It is calculated with Equation 5.8.

$$F_{b,Rd} = \frac{k_1 \alpha_b f_u d t}{\gamma_{M2}} \quad (5.8)$$

Where

$F_{b,Rd}$	Bearing resistance
k_1	Factor representing bolt placement, $k_1 = 2.5$
α_b	Reduction factor, $\alpha_b = 1$ where the shear plane passes through the unthreaded portion of the bolt
f_u	Ultimate strength of the material which is joined by the bolt
d	Nominal diameter of the bolt
t	Thickness of the plate
γ_{M2}	Partial safety factor for joints, $\gamma_{M2} = 1.25$

By modifying Equation 5.8, the required thickness of the plate can be expressed, as shown in Equation 5.9.

$$t_{req} = \frac{F_{h,d} \gamma_{M2}}{K_1 \alpha_b f_u d} \quad (5.9)$$

For several types of bolts, values of t_{req} are shown in Table 5.4.

Table 5.4: Required thickness, t_{req} , of plates to fulfill bearing resistance

Lateral stiffener	M8	M10	M12	M14	M16
L1	8.4mm	6.7mm	5.6mm	4.8mm	4.2mm
L2	16.7mm	13.4mm	11.1mm	9.5mm	8.4mm
L3	25.1mm	20mm	16.7mm	14.3mm	12.5mm
L4	33.4mm	26.7mm	22.3mm	19.1mm	16.7mm

Based on the results obtained in this Section, the design of the type 1 connection is summarized in Table... The thicknesses of the plates which are directly connected to the lateral stiffeners are set equal to the thickness of the stiffeners, in order to eliminate stress concentrations due to necking. Thickness of the plate on top of the Floor element is set to 30mm, which corresponds to thickness of the extruded edge sheet used for production of the floor element.

Table 5.5: Design of the type 1 connection

Lateral stiffener	Bolt C1	Bolts C2 and C3	t_c, t_s	t_f
L1	M14	M10	15mm	30mm
L2	M14	M12	30mm	30mm
L3	M14	M14	45mm	30mm
L4	M14	M16	60mm	30mm

5.1.2 Type 2 connection

Type 1 connection is designed to join floor element, column and lateral stiffeners L5 and L5, which contain steel bracing rods.

Figures 5.5 and 5.6 show side-view sections of the Type 1 connection which is linking roof, column and lateral stiffeners L1 to L4. Figure 5.7 shows top-view section of the connection and Figure 5.8 view from the bottom.

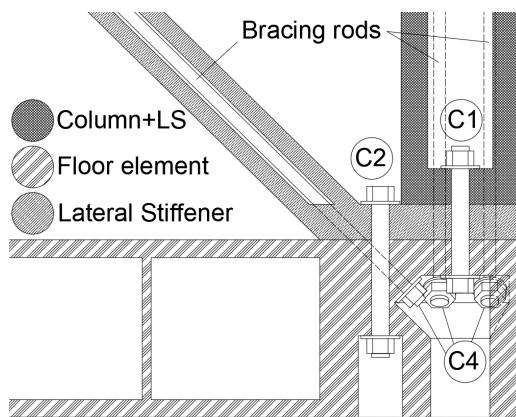


Figure 5.5: A-A' side-view section of the type 2 connection

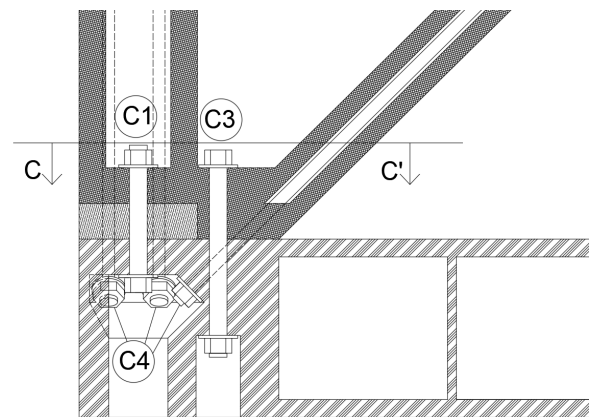


Figure 5.6: B-B' side-view section of the type 2 connection

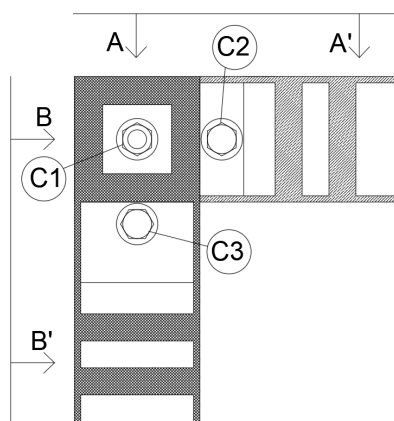


Figure 5.7: C-C' top-view section of the type 2 connection

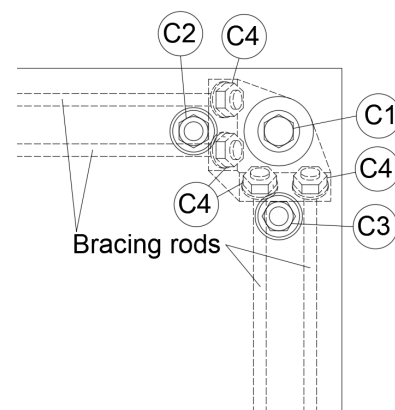


Figure 5.8: Bottom-view of the type 2 connection

Bolts C1, C2 and C3 are same as in the case of type 1 connection which joins lateral stiffeners L4. This is due to the fact that the cross-sectional area of the plastic part of stiffeners L5 and L6 is

same as the cross-sectional area of stiffener L4. The excessive tensile force is carried by steel bracing rods.

In the same way as in the previous Section, the maximum forces in the steel bracing rods can be calculated by reversing process described by Equations 4.20 to 4.23. Then by multiplying these values by force factor $\gamma_f = 1.5$, design values of the tensile forces in the bracing rods are obtained. The results are presented in Table 5.6.

Table 5.6: Maximal forces acting on the bracing rods

Bracing rod	N_{max} [kN]	N_d [kN]	d_w [mm]	$t_{p,req}$ [mm]
ø6mm	5.81	8.71	8	16.8
ø8mm	10.33	15.49	10	23.9
ø12mm	23.24	34.86	14	38.4
ø16mm	41.31	61.97	24	39.8
ø20mm	64.55	96.83	28	53.3
ø24mm	92.96	139.44	36	59.7
ø27mm	117.65	176.47	46	59.2
ø30mm	145.25	217.87	56	60

The tension resistance of the bracing rods is inherently satisfied. However, the punching shear resistance, Equation 5.4, needs to be checked. Due to construction reasons, the thickness of the plate resisting punching is limited to 60mm. Then, with use of Equation 5.5, the diameters of the washers, d_w , supporting fastening nuts can be determined. The results are presented in Table 5.6. It can be seen that 60mm thickness of the supporting plate can safely support all the bracing rods without necessity of excessively big washers.

5.2 Inter-module connections

The purpose of inter-module connections is to join adjacent modules. A detail of such connection which is connecting two modules on top of each other is shown on Figure 5.9. The main load-bearing component of the joint is the connecting rod.

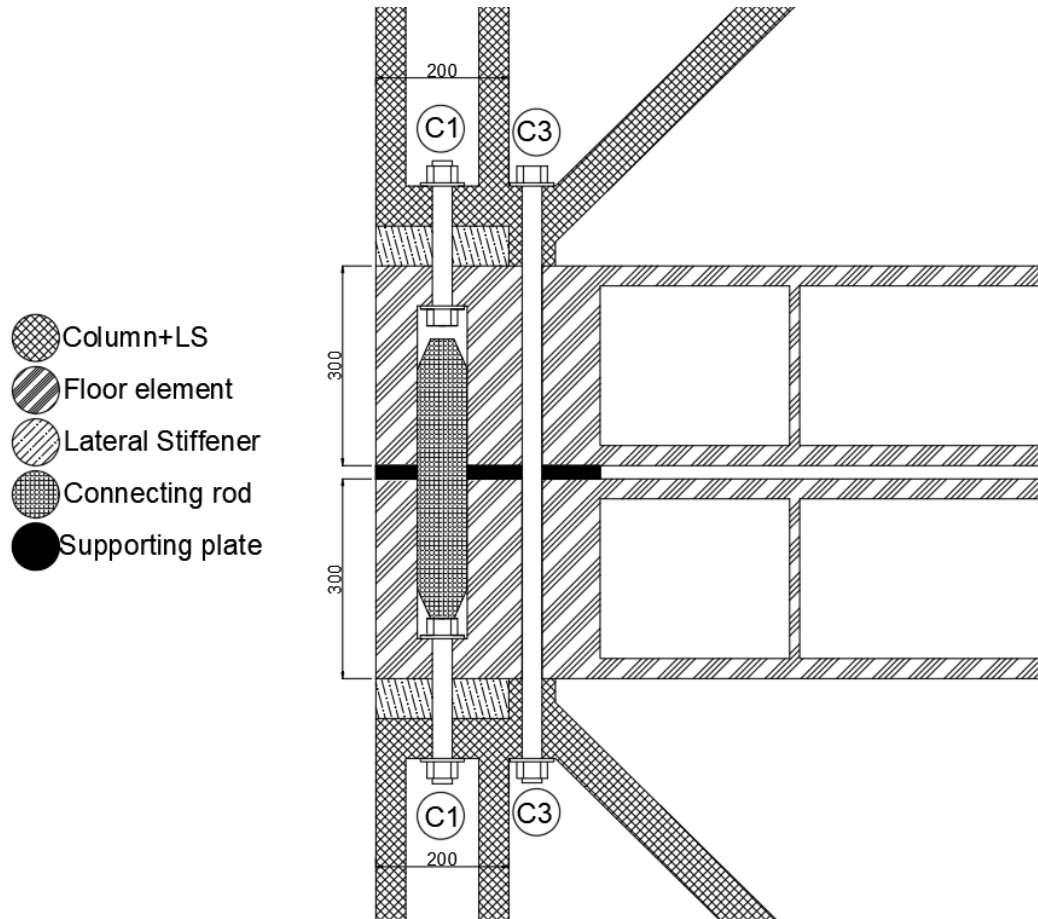


Figure 5.9: Inter-module connection joining two modules on top of each other

Bolts C2 and C3 have just controlling function. They are using the same holes as the bolts described in Section 5.1 as intra-module connections. When a module is to be placed into the building, the intra-module connections C2 and C3 are left disjointed. After they are incorporated into the building, the connections are assembled.

The main load-bearing component of the inter-module joint is the connecting rod on Figure 5.9. The material of rod is POM. However, it is extrusion molded and therefore the ultimate strength of the material is $f_{ub} = 67\text{MPa}$. It is only capable to carry shear forces. Its shear resistance can be calculated with Equation 5.10.

$$F_{v,Rd} = \frac{\alpha_v f_{ub} A}{\gamma_{M2}} \quad (5.10)$$

Where

$F_{v,Rd}$		Shear resistance per shear plane
α_v		Reduction factor, $\alpha_v = 0.6$
f_{ub}		Ultimate strength of the rod, $f_{ub} = 67\text{MPa}$
A		The gross cross-section of the connecting rod
γ_{M2}		Partial safety factor for joints, $\gamma_{M2} = 1.25$

After applying values the Equation 5.10 yields:

$$F_{v,Rd} = \frac{0.6 * 67\text{MPa} * 4.42 * 10^{-3}\text{m}^2}{1.25} = 142.076\text{kN} \quad (5.11)$$

Further, bearing resistance of the connecting need to be calculated:

$$F_{b,Rd} = \frac{k_1 \alpha_b f_u d t}{\gamma_{M2}} \quad (5.12)$$

Where

$F_{b,Rd}$		Bearing resistance
k_1		Factor representing bolt placement
α_b		Reduction factor
f_u		Ultimate strength of the material which is joined by the rod
d		Nominal diameter of the rod
t		Thickness of the plate
γ_{M2}		Partial safety factor for joints, $\gamma_{M2} = 1.25$

$$k_1 = 2.8 \frac{e_2}{d_0} - 1.7 = 0.633 \quad (5.13)$$

Where

e_2		Distance of the rod from the edge
d_0		Nominal diameter of the rod

After solving for Equation 5.14 we obtain:

$$F_{b,Rd} = \frac{0.633 * 0.278 * 67\text{MPa} * 0.075\text{m} * 0.2\text{m}}{1.25} = 141.483\text{kN} \quad (5.14)$$

These calculations indicate that the designed inter-module connection has higher resistance to shear forces than is the largest occurring wind load acting on any single unit, calculated in Section 3.5. The design is preliminarily considered safe. However, further investigation is needed, especially in verification of dynamic behavior of the connection and its influence on structural behavior.

Further, Figure 5.10 shows the same type of connection joining 4 modules. Same characteristic apply also for this version. The connection is capable also to connect 8 modules and to join the 1st storey modules to the foundation.

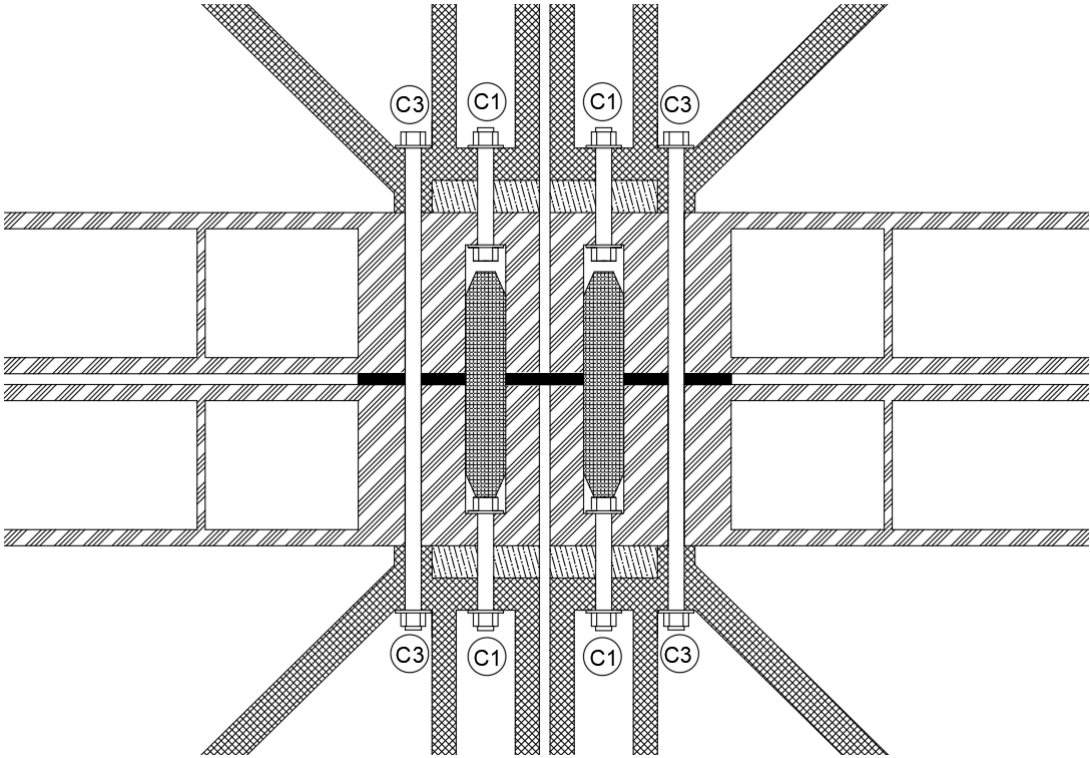


Figure 5.10: Inter-module connection joining four modules

Conclusion 6

The aim of this theses was to explore adoption of advanced manufacturing into the construction industry, to move further towards sustainability of the Earth's environment and tackle the problem of scarcity of affordable housing.

Innovative production technology was introduced, which combines continual extrusion and additive manufacturing. Used material was up-cycled industrial waste plastic, more specifically polyoxymethylene (POM), an engineering plastic with relatively low sensitivity to creep and high temperatures. Its advantages are high durability and workability. Furthermore, at the end of the lifetime the material can be reused and recycled.

Corner supported modular system with stiff modules was adopted to design case multi-story modular buildings. The modules of the buildings are fully produced, assembled and outfitted off-site, in controlled environment. This allow mass production and mass customization of the modules, which decreases manufacturing costs. More affordable houses of superior quality can be produced. Moreover, the whole building is modular and can be disassembled in the same way in which it was assembled.

Load acting on the structures were calculated and their effects analysed. Based on that, structural elements were designed. Emphasis was put into stiffness of the structure, due to relatively low stiffness of the POM material. Due to that, most of the structural material was not used effectively. This is favorable as robust structure is needed while effects of the production technology on the used material are unknown.

For taller buildings, steel bracing rods were used to provide required structural stiffness. The production technology allows creation of internal channels into which the bracing rods can be inserted. They connect corners of the stiff modules, where they are anchored with use of nuts and washers. The stiff modules provide lateral stability and stiffness for the whole building.

Joints between the structural elements and modules were designed so they allow complete disassembly. This provides a benefit that the modules can be reused, used as self-standing structures, reallocated and at the end of the lifetime easily recycled. This system can react to fluctuations of demand and provide temporary housing in times of crisis.

Bibliography

- Crawford, 1998.** R. J Crawford. *Plastics Engineering 3rd Edition*. ISBN 9780750637640. Butterworth-Heinemann, paperback edition, 1998.
- CTF, 1998.** Construction Task Force CTF. *Rethinking Construction*, 1998.
- EN1990:2002, 2010.** EN1990:2002. *EN 1990:2002*. 978 0 580 71374 3. Standards Policy and Strategy Committee, e-book edition, 2010.
- EN1991-1-1:2002, 2010.** EN1991-1-1:2002. *EN 1991-1-1:2002*. 978 0 580 66415 1. Standards Policy and Strategy Committee, e-book edition, 2010.
- EN1991-1-3:2003, 2010.** EN1991-1-3:2003. *EN 1991-1-3:2003*. 978 0 580 66413 7. Standards Policy and Strategy Committee, e-book edition, 2010.
- EN1991-1-4:2005, 2013.** EN1991-1-4:2005. *EN 1991-1-4:2005*. 978 0 580 80738 1. Standards Policy and Strategy Committee, e-book edition, 2013.
- EN1991-1-4:2007, 2007.** EN1991-1-4:2007. *EN 1991-1-4:2007*. 0 580 45959 4. Standards Policy and Strategy Committee, e-book edition, 2007.
- EN1991-1-8:1992, 2005.** EN1991-1-8:1992. *EN 1993-1-8:1992*. 978 0 580 72497 8. Standards Policy and Strategy Committee, e-book edition, 2005.
- Gibb, 1999.** Alistair G.E Gibb. *Off-site Fabrication: Prefabrication, Pre-assembly and Modularisation*. ISBN 978-1-84995-289-7. Whittles Publishing, e-book edition, 1999.
- Jensen, 2015.** Thomas Brunoe Jensen, Kjeld Nielsen. *Application of Mass Customization in the Construction Industry*, 2015.
- Lawson, 2014.** Chris Goodier Lawson, Ray Ogden. *Design in Modular Construction*. ISBN 978-0-203-87078-5. CRC Press, e-book edition, 2014.
- Lüftl, 2014.** Sarath Chandran Lüftl, Visakh P.M. *Polyoxymethylene Handbook: Structure, Properties, Applications and Their Nanocomposites*. ISBN 978-1-118-38511-1. Scrivener Publishing, e-book edition, 2014.
- Sung-Hoon, 2002.** Dan Odell Shad Roundy Paul K. Wright Sung-Hoon, Michael Montero. *Anisotropic material properties of fused deposition modeling ABS, Rapid Prototyping Volume 8 · Number 4 · 2002 · pp. 248–257*, 2002.
- Troughton, 2008.** M.J. Troughton. *Handbook of plastics joining : a practical guide - 2nd ed.* ISBN 978-0-8155-1581-4. William Andrew Inc., e-book edition, 2008.
- WEF, 2016.** World Economic Forum WEF. *Shaping the Future of Construction: A Breakthrough in Mindset and Technology*, 2016.

Part I

Appendix

POM Datasheet



TECAFORM AH natural - Stock Shapes

Chemical Designation
POM-C (Polyacetal (Copolymer))

Colour
white opaque

Density
1.41 g/cm³

Main features
→ high strength
→ resistant to cleaning agents
→ stiff
→ high toughness
→ very good electrical insulation
→ good machinability
→ good slide and wear properties
→ difficult to bond

Target Industries
→ mechanical engineering
→ automotive industry
→ aircraft and aerospace technology
→ electronics
→ food technology
→ oil and gas industry
→ medical technology

Mechanical properties	parameter	value	unit	norm	comment
Modulus of elasticity (tensile test)	1mm/min	2800	MPa	DIN EN ISO 527-2	1)
Tensile strength	50mm/min	67	MPa	DIN EN ISO 527-2	
Tensile strength at yield	50mm/min	67	MPa	DIN EN ISO 527-2	
Elongation at yield	50mm/min	9	%	DIN EN ISO 527-2	
Elongation at break	50mm/min	32	%	DIN EN ISO 527-2	
Flexural strength	2mm/min, 10 N	91	MPa	DIN EN ISO 178	2)
Modulus of elasticity (flexural test)	2mm/min, 10 N	2600	MPa	DIN EN ISO 178	
Compression strength	1% / 2% / 5% 5mm/min, 10 N	20/35/68	MPa	EN ISO 604	3)
Compression modulus	5mm/min, 10 N	2300	MPa	EN ISO 604	4)
Impact strength (Charpy)	max. 7.5J	n.b.	kJ/m ²	DIN EN ISO 179-1eU	5)
Notched impact strength (Charpy)	max. 7.5J	8	kJ/m ²	DIN EN ISO 179-1eA	
Ball indentation hardness		165	MPa	ISO 2039-1	6)
Thermal properties	parameter	value	unit	norm	comment
Glass transition temperature		-60	°C	DIN EN ISO 11357	1)
Melting temperature		166	°C	DIN EN ISO 11357	
Service temperature	short term	140	°C		2)
Service temperature	long term	100	°C		
Thermal expansion (CLTE)	23-60°C, long.	13	10 ⁻⁵ K ⁻¹	DIN EN ISO 11359-1;2	
Thermal expansion (CLTE)	23-100°C, long.	14	10 ⁻⁵ K ⁻¹	DIN EN ISO 11359-1;2	
Specific heat		1.4	J/(g*K)	ISO 22007-4:2008	
Thermal conductivity		0.39	W/(K*m)	ISO 22007-4:2008	
Electrical properties	parameter	value	unit	norm	comment
Specific surface resistance	Silver electrode, 23°C, 12% r.h.	10 ¹⁴	Ω	DIN IEC 60093	1)
Specific volume resistance	Silver electrode, 23°C, 12% r.h.	10 ¹³	Ω*cm	DIN IEC 60093	2)
Dielectric strength	23°C, 50% r.h.	49	kV/mm	ISO 80243-1	2)
Resistance to tracking (CTI)	Platin electrode, 23°C, 50% r.h., solvent A	600	V	DIN EN 60112	
Other properties	parameter	value	unit	norm	comment
Water absorption	24h / 96h (23°C)	0.05 / 0.1	%	DIN EN ISO 62	1)
Resistance to hot water/ bases		(+)	-	-	2)
Resistance to weathering		-	-	-	3)
Flammability (UL94)	corresponding to	HB	-	DIN IEC 60695-11-10;	4)

Our information and statements reflect the current state of our knowledge and shall inform about our products and their applications. They do not assure or guarantee chemical resistance, quality of products and their merchantability in a legally binding way. Our products are not defined for use in medical or dental implants. Existing commercial patents have to be observed. The corresponding values and information are no minimum or maximum values, but guideline values that can be used primarily for comparison purposes for material selection. These values are within the normal tolerance range of product properties and do not represent guaranteed property values. Therefore they shall not be used for specification purposes. Unless otherwise noted, these values were determined by tests at reference dimensions (typically rods with diameter 40-80 mm according to DIN EN 15860) on extruded and machined specimen. As the properties depend on the dimensions of the semi-finished products and the orientation in the component (esp. in reinforced grades), the material may not be used without a separate testing under individual circumstances. The customer is solely responsible for the quality and suitability of products for the application and has to test usage and processing prior to use. Data sheet values are subject to periodic review, the most recent update can be found at www.ensinger-online.com. Technical changes reserved.

Ensinger GmbH
Rudolf-Diesel Str. 8
71154 Nufringen - Deutschland

Tel +49 7032 819 0
Fax +49 7032 819 100
ensingerplastics.com

Date: 2018/02/20

Version: AD

Creep curves for POM B

Figure B.1 represent creep of POM and nanocomposites of POM at temperature 30 °C, obtained from Lüftl [2014]. Figures B.2 and B.3 show creep curves of POM material at ambient temperature 20 °C, obtained from Crawford [1998]. They represent dependency of the strain on the time period of application of a given stress in the material.

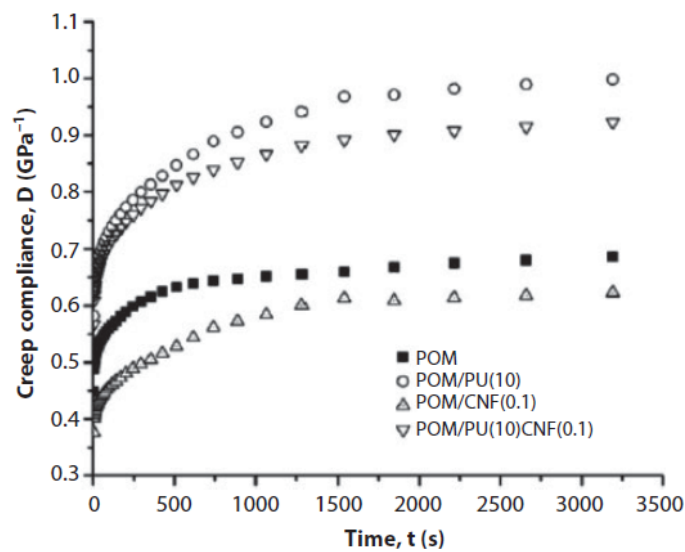


Figure B.1: Creep of POM (squares) and nanocomposites of POM

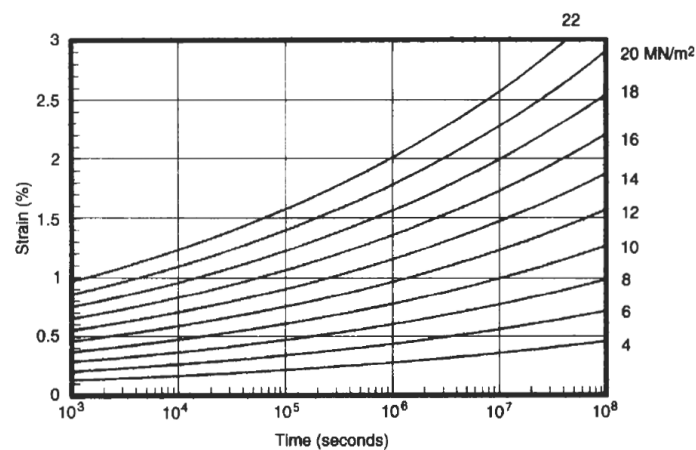


Figure B.2: Creep curves for POM, time in seconds

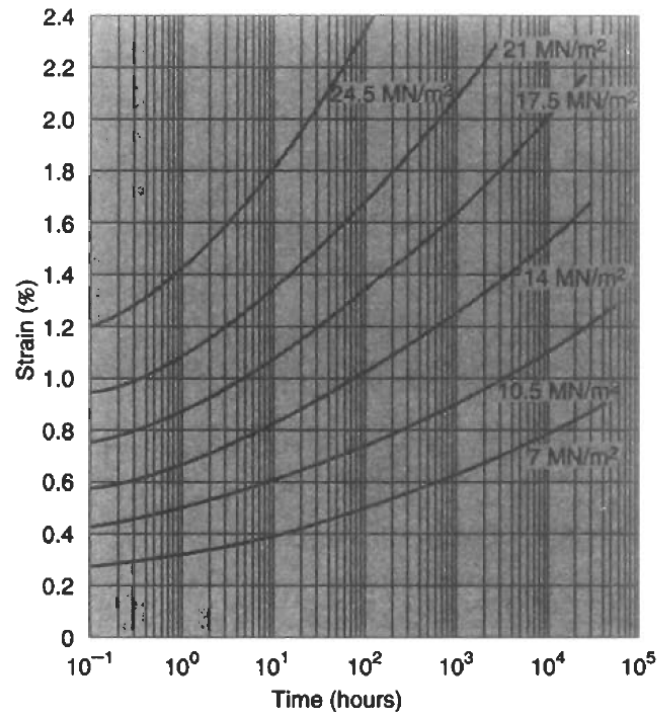


Figure B.3: Creep curves for POM, time in hours

Wind Loads C

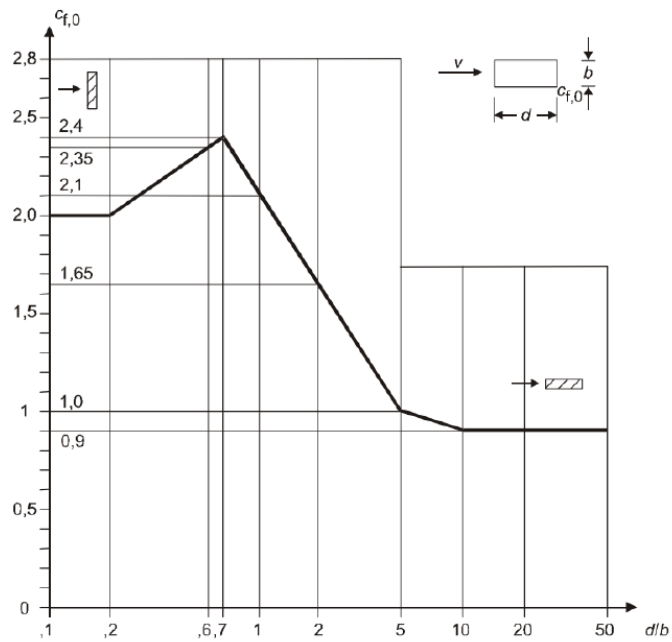


Figure C.1: Graph for determination of the force coefficient of rectangular sections, $c_{f,0}$, with sharp corners and without free-end flow

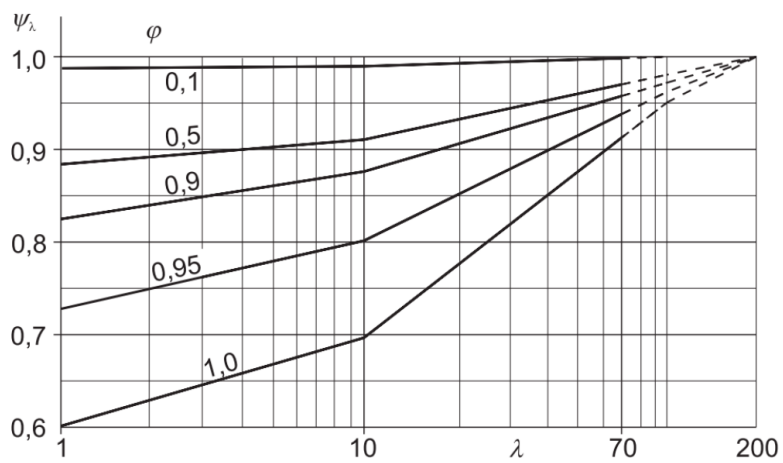


Figure C.2: Graph for determination of the end-effect factor

No.	Position of the structure, wind normal to the plane of the page	Effective slenderness λ
1	<p>for $b \leq l$</p>	<p>For polygonal, rectangular and sharp edged sections and lattice structures:</p> <p>for $\ell \geq 50$ m, $\lambda = 1,4 \ell/b$ or $\lambda = 70$, whichever is smaller</p>
2	<p>$b_1 \leq 1,5b$</p> <p>$b_1 \leq 1,5b$</p> <p>$b \leq l$</p> <p>$b_0 \geq 2,5b$</p>	<p>for $\ell < 15$ m, $\lambda = 2 \ell/b$ or $\lambda = 70$, whichever is smaller</p> <p>For circular cylinders:</p> <p>for $\ell \geq 50$, $\lambda = 0,7 \ell/b$ or $\lambda = 70$, whichever is smaller</p> <p>for $\ell < 15$ m, $\lambda = \ell/b$ or $\lambda = 70$, whichever is smaller</p>
3	<p>$\frac{l}{2}$</p> <p>$\frac{b}{2}$</p> <p>b</p> <p>l</p>	<p>For intermediate values of ℓ, linear interpolation should be used</p>
4	<p>$b_1 \geq 2,5b$</p> <p>b</p> <p>l</p> <p>l</p> <p>b</p> <p>$z_g \geq 2b$</p>	<p>for $\ell \geq 50$ m, $\lambda = 0,7 \ell/b$ or $\lambda = 70$, whichever is larger</p> <p>for $\ell < 15$ m, $\lambda = \ell/b$ or $\lambda = 70$, whichever is larger</p> <p>For intermediate values of ℓ, linear interpolation should be used</p>

Figure C.3: Table for determination of the slenderness of the building